REPUBLIC OF TÜRKİYE
AYDIN ADNAN MENDERES UNIVERSITY
GRADUATE SCHOOL OF NATURAL AND APPLIED SCIENCES
DEPARTMENT OF MECHANICAL ENGINEERING
MASTER'S PROGRAMME IN MECHANICAL ENGINEERING
2024-MSc-101

DISC BRAKE DESIGN AND ANALYSIS WITH FINITE ELEMENT METHODS

Emre CEYLAN

MASTER'S THESIS

SUPERVISOR

Prof. Dr. Ismail BOGREKCI

AYDIN–2024

ACCEPTANCE AND APPROVAL

The thesis titled “DISC BRAKE DESIGN AND ANALYSIS WITH FINITE ELEMENT METHODS”, prepared by Emre CEYLAN, a student of Department of Mechanical Engineering Program at Republic of Türkiye Aydın Adnan Menderes University, Graduate School of Natural and Applied Science, was accepted as a Master's Thesis by the jury below.

Date of Thesis Defense: 12/11/2024

Jury Member

APPROVAL:

Chair (Supervisor) : Prof. Dr. Ismail BOGREKCI
Aydin Adnan Menderes University

Member : Prof. Dr. Pinar DEMIRCIOGLU
Aydin Adnan Menderes University

Member : Assoc. Prof. Dr. Salih OZER
Mus Alparslan University

This thesis was approved by the jury above in accordance with the relevant articles of the Aydın Adnan Menderes University Graduate Education and Examination Regulations and was approved on the …… by from the Board of Directors of the Graduate School of Science in the …… numbered decision.

Prof. Dr. Ethem AKTURK

Institute Director

Dedicated to my beloved family.

ACKNOWLEDGEMENTS

I would like to thank my advisor, Prof. Dr. ISMAIL BOGREKCI, who showed his trust in me throughout my thesis and took a close interest in my work. I would like to convey my endless respects to my esteemed teacher Prof. Dr. PINAR DEMIRCIOGLU, who guided me with his advice and spared time for me in my studies.

I would like to express my endless thanks to my close friends and family who always motivate me.

Sincerely,

Emre CEYLAN

SCIENTIFIC ETHICS STATEMENT

I hereby declare that I composed all the information in my Master's/Doctoral thesis entitled "DISC BRAKE DESIGN AND ANALYSIS WITH FINITE ELEMENT METHODS" within the framework of ethical behavior and academic rules, and that due references were provided and for all kinds of statements and information that do not belong to me in this study in accordance with the guide for writing the thesis. I declare that I accept all kinds of legal consequences in case of any contrary statement of what I have stated is revealed.

……..

Emre CEYLAN

… / … /

TABLE OF CONTENTS

LIST OF ABBREVAITIONS

2D: Two Dimensional

3D: Three Dimensional

CAD: Computer Aided Design

FEA: Finite Element Analysis

ISO: International Organization of Standardization

MPa: Megapascal

RPM: Revolution Per Minute

FEM: Finite Element Method

LIST OF FIGURES

LIST OF TABLES

ÖZET

DİSK FREN TASARIMI VE SONLU ELEMANLAR METHODU İLE ANALİZİ

Ceylan E. Aydın Adnan Menderes Üniversitesi, Fen Bilimleri Enstitüsü, Makine Mühendisliği Anabilim Dalı Yüksek Lisans Programı, Yüksek Lisans Tezi, Danışman: Prof. Dr. İsmail Böğrekci, Aydın, 2024.

Bu tez ile, fren sistemlerinde kullanılan disk frenin tasarımı ve bu tasarımın bilgisayar destekli mühendislik hesaplama araçları kullanılarak optimum tasarımın elde edilmesi amaçlanmaktadır. Optimum tasarım için disk fren tasarımında hem disk geometrisi hem de diskin malzeme kalitesi değiştirilerek optimum tasarıma ulaşmak hedeflenmektedir.

Bu tezde, tasarım ve optimizasyon için bilgisayar destekli mühendislik hesaplama araçları kullanılarak disk fren tasarımının verimliliğinin arttırılması hedeflenmiştir. Bu hedefe ulaşmak için, tasarım oluşturulmuş ve sonlu elemanlar metodu ile analiz yöntemleri kullanılmıştır.

Bu tezde, tasarım geometrisi ve malzeme kalitesi değiştirilerek, termal iletkenlik kıyaslanmış, en verimli disk geometrisinin ve malzeme kalitesinin belirlenmesi amaçlanmıştır. Alüminyum alaşımlı çelik, paslanmaz çelik ve yapı çeliği kullanarak malzeme kalitesi değiştirilmiştir. Bu farklı tasarımlar karşılaştırılarak tasarım parametrelerinin sonuçlara etkileri değerlendirilmiştir.

Bu çalışmanın sonuçlarının, disk fren tasarımı ve malzeme kalitesi seçimi ile termal iletkenlik performansı arasındaki ilişkiye dair önemli öngörüler sağlaması beklenmektedir.

Anahtar Sözcükler: Disk, Fren, Balata, Kaliper, Disk geometrisi, Termal iletkenlik verimliliği, FEA, Sonlu elemanlar metodu ile analiz, Optimizasyon

ABSTRACT

DISC BRAKE DESIGN AND ANALYSIS WITH FINITE ELEMENT METHODS

Ceylan E. Aydin Adnan Menderes University, Graduate School of Natural and Applied Sciences, Department of Mechanical Engineering Master's Programme, Master's Thesis, Supervisor: Prof. Dr. Ismail BOGREKCI, Aydin, 2024.

The main objective of this thesis is aimed to design the disc brake used in braking systems and to obtain the optimum design by using computer-aided engineering calculation tools. For optimum design, it is aimed to reach the optimum design by changing both the disc geometry and the material quality of the disc in disc brake design.

In this thesis, it is aimed to increase the efficiency of disc brake design by using computer-aided engineering calculation tools for design and optimization. To achieve this goal, the design was created, and the finite element method and analysis methods were used.

In this thesis, thermal conductivity was compared by changing the design geometry and material quality and it was aimed to determine the most efficient disk geometry and material. The material quality has been changed by using aluminum alloy steel, stainless steel and structural steel. By comparing these different designs, the effects of the design parameters on the results were evaluated.

The results of this study are expected to provide important insights into the relationship between disc brake design and material quality selection and thermal conductivity performance.

Keywords: Disc, Brake, Pad, Caliper, Disc geometry, Thermal conductivity efficiency, FEA, Analysis with finite element method, Optimization

1. INTRODUCTION

In the automotive industry, which grows day by day, competition and the performance of vehicles gain great importance. Braking systems are also included among the performance criteria. The brake system is also one of the most important systems in vehicles in terms of safety. The main purpose of the braking system is to slow down or stop the rotation of the wheel. The disc brake system is just one of these brake systems.

The disc brake system consists of brake disc, brake caliper, brake pads, brake piston and sealing elements. The brake disc is mounted on the axle. The wheel is mounted on the axle. Brake pads are used as friction plates. Brake pads are located inside the brake caliper. By rubbing the brake disc on both surfaces through the pads, the brake disc is enabled to slow down or stop the wheel. In this working principle, the brake pads inside the brake caliper can be driven mechanically, hydraulically, pneumatically or electromagnetically.

In the disc brake system, friction force occurs between the surfaces rubbing against each other to reduce the movement. Due to this force, the brake disc becomes hot. At this point, brake disc design and material quality become important. Heat transfer rate is an important factor for the time spent cooling the brake disc. The greater the surface area where the brake disc and pads rub, the lower the heat transfer rate. In brake discs with the same friction surface area, ventilation channels are opened on the brake disc to provide more efficient cooling. This type of brake discs is widely used in automobile braking systems.

In order to increase the efficiency and optimization of the disc brake system, better braking performance can be obtained by analyzing it with the finite element method. For this purpose, the optimum brake disc can be determined by changing the design geometry and material quality and comparing the results in terms of design criteria such as thermal conductivity, heat transfer and strength.

Moreover, keeping up with regular maintenance and timely replacing worn-out brake components are vital for ensuring your braking system lasts and stays reliable. As you drive, your brake pads and discs naturally wear down from all the friction, which can reduce how well your brakes work and make it take longer to stop. By checking these parts regularly and replacing them when needed, you can prevent brake failures and keep your vehicle safe.

Today’s advances in sensor technology and diagnostics make it easier to monitor the health of your brake system, giving you a heads-up about potential problems before they get serious.

In addition, the addition of advanced braking technologies like anti-lock braking systems (ABS) and electronic stability control (ESC) has significantly boosted vehicle safety. These systems work alongside traditional disc brakes to give you better control and stability during emergency stops. ABS stops your wheels from locking up, so you keep traction and can still steer, while ESC helps you stay on course. As car technology keeps advancing, improving braking systems will remain a top priority to ensure both safety and top-notch performance in the ever-competitive automotive market.

2. LITERATURE REVIEW

Many researchers have explored the workings of disc brake systems, providing valuable insights into their components and operation. For example, Dr. Suresh, in a study from 2013, described how disc brakes are used to slow down or stop a vehicle's wheels. He explained that the system includes a rotor (or disc), caliper, pads, pistons, and sealing elements. Hydraulic oil in the caliper moves the pistons, which then push the brake pads against the disc. This action creates friction, which slows down or stops the vehicle. This is the basic idea behind how disc brake systems work.

Cheatan Kumar Yadav and U. K. Joshi, in their 2018 study, explained how disc brakes work and their benefits. A disc brake uses calipers to squeeze pairs of pads against a disc or rotor, creating friction that slows down or stops the rotation of a vehicle's axle. This process converts the vehicle's motion into heat, which needs to be dispersed to prevent overheating.

The brake disc, or rotor, is the part that rotates with the wheel and is typically made of gray iron, a type of cast iron. Disc designs vary; some are solid, while others are ventilated with fins or vanes to help cool the brakes more efficiently. Ventilated discs are especially useful for heavier vehicles or those that require high braking power, as they dissipate heat better and prevent brake fade. This is particularly important in situations like driving down a steep hill or during repeated high-speed stops, where drum brakes might fail. Another advantage of disc brakes is their consistent performance, as the braking force is directly proportional to the friction between the pads and the rotor.

In this thesis, different materials such as aluminum alloy steel, stainless steel, and structural steel were selected for the brake disc. The work will focus on these materials to analyze their performance. However, various brake disc designs have been created using different material qualities. According to Shaik and Srinivas (2012) and Nathil (2013), disc brakes are usually made from cast iron or ceramic composites that include carbon, Kevlar, and silica. These discs are connected to the wheel and axle to stop the vehicle. A friction material in the form of brake pads is applied to both sides of the disc through mechanical, hydraulic, pneumatic, or electromagnetic means. In this study, a hydraulically driven system designed to operate under a specific pressure will be used. The friction generated by this system causes the disc and attached wheel to slow down or stop.

Dr. Suresh (2013), Reddy (2013), and Joseph (2017) have noted that vehicles generally use methodologies like regenerative braking and friction braking systems. A friction brake works by generating frictional forces when two or more surfaces rub against each other to reduce movement. Depending on the design, vehicle friction brakes can be categorized into drum and disc brakes.

Cheatan Kumar Yadav and U. K. Joshi, in their 2018 study, presented a table comparing the mechanical properties of various materials used for brake discs, including cast iron alloy, titanium alloy, Al-Ni-Co alloy, and structural steel alloy. This table highlights the differences in maximum von Mises stress, maximum total deformation, and weight reduction between Al-Ni-Co alloy, titanium alloy, and cast iron. By evaluating these factors, the researchers determined the most suitable material for brake discs based on total deformation, stress, strain, weight, and other properties.

The study concluded that both Al-Ni-Co alloy and titanium alloy are superior choices for brake discs compared to cast iron and structural steel. These materials demonstrated better performance in terms of lower total deformation and stress while also offering significant weight reduction. This makes them ideal for use in high-performance and lightweight automotive applications, where reducing weight without compromising strength and durability is crucial.

Table 2.1. Mechanical properties of materials

Properties	Cast Iron Alloy	Titanium Alloy	AL-NI-CO Alloy	Structural Steel Alloy
Total Deformation (mm)	0.0151	0.025	0.012	0.017
Equilavent Stress (MPa)	75.48	73.725	73.099	74.123
Equilavent Elastic Strain	0.00047	0.00078	0.00031	0.00037
Factor of Safety	3.71	12.613	9.5	3.3
Temperature (°C)	85	75.26	87.5	80
Heat Flux (W/mm²)	0.4	0.188	0.161	0.57
Weight (kg)	3	1.5	2.84	3.2

Guru Murty Nathi, T. N. Charyulu, K. Gowtham, and P. Satish Reddy, in their 2012 study, highlighted the finite element method (FEM) as a powerful tool for obtaining

numerical solutions to a wide range of engineering problems. The versatility of FEM allows it to handle complex shapes and geometries for any material under various boundaries and loading conditions. This adaptability makes FEM particularly suitable for analyzing today's intricate engineering systems and designs, where traditional closed-form solutions for governing equilibrium equations are often unavailable.

Moreover, FEM serves as an efficient design tool, enabling designers to conduct parametric design studies by evaluating different shapes, materials, and loads. This allows for a comprehensive analysis of various design scenarios, helping to identify the optimal design. The ability to simulate and analyze multiple design cases makes FEM invaluable for modern engineering, where precision and optimization are critical.

Dr. Suresh, in his 2013 study, emphasized the importance of thermal characteristics in disc brakes. He explained that solid-body disc brakes have a lower heat transfer rate, resulting in slower cooling times. This is because solid discs have a larger contact area between the disc and brake pads. In contrast, ventilated discs are extensively used in automotive braking systems to enhance cooling efficiency during braking.

Ventilated discs maintain the same contact area between the disc and pads, but they incorporate ventilation channels or fins between the friction surfaces. These channels facilitate better airflow and heat dissipation, allowing the disc to cool more effectively. This design feature is particularly beneficial in high-performance or heavy-duty applications where brake systems are subjected to repeated or prolonged braking, preventing overheating and maintaining consistent braking performance. Therefore, while solid discs offer simplicity and durability, ventilated discs are preferred in demanding automotive environments for their superior thermal management capabilities.

F. Talati and S. Jalalifar, in their 2008 study, highlighted the significant thermal stresses that disc brakes endure during both regular and hard braking. They noted that routine braking and sudden, high-deceleration events typical of passenger vehicles can lead to extreme temperatures, sometimes reaching up to 900°C in a very short time span.These rapid temperature changes can result in thermal shock, which may cause surface cracks on the brake rotor. Alternatively, under conditions where thermal shock is absent, the repetitive application of high deceleration forces can induce macroscopic cracks that propagate through the thickness and along the radius of the disc brake. This phenomenon indicates the substantial mechanical challenges that brake rotors face under demanding operational conditions.

Understanding the complex interplay of thermal and mechanical stresses is paramount in the design of brake systems capable of enduring extreme conditions without sacrificing safety or performance. Engineers must carefully select materials that can withstand high temperatures and rapid temperature changes, such as those experienced during hard braking. Additionally, effective cooling mechanisms, whether through ventilated designs or advanced cooling fluids, play a crucial role in dissipating heat and preventing thermal shock-induced damage or material fatigue. Moreover, the structural design of disc brakes must be robust enough to handle the repetitive high-g decelerations typical of everyday driving and emergency situations. This includes optimizing the geometry and thickness of the brake rotor to resist thermal deformation and minimize the risk of cracking under stress. By integrating these considerations into the design process, engineers can enhance the durability and reliability of disc brake systems across a wide range of automotive applications, ensuring consistent performance and safety for vehicle operators and passengers alike.

Ali Belhocine and Mostefa Bouchetara, in their 2012 study, explored the thermal behavior of dry contacts in brake discs. They emphasized that thermal analysis is a crucial aspect of studying brake systems because the temperature directly influences the thermomechanical behavior of the brake disc structure. During braking, the temperatures and thermal gradients are extremely high, leading to significant stress and deformation, which can cause cracks to form and worsen over time. Therefore, accurately determining the temperature field of the brake disc is essential. In the braking phase, the temperature does not have sufficient time to stabilize in the disc, making a transient analysis necessary. Evaluating the thermal gradients also requires a three-dimensional model of the problem. The thermal loading is modeled as a heat flux entering the disc through the brake pads. Ventilated discs, commonly used in automotive brake systems, must have rapid cooling capabilities and a robust structural design to prevent thermal deformation, as their temperatures soar during braking. A disc with effective cooling performance can manage its temperature rise, thereby preventing thermal issues such as hot judder, which occurs due to thermal deformation of the disc. In braking systems, mechanical energy is converted into thermal energy, leading to the heating of the disc and pads. This energy dissipation results in temperature increases ranging from 300°C to 800°C. The heat in the contact area is primarily due to plastic micro-deformations caused by the friction forces. Understanding these thermal dynamics is crucial for designing brake systems that maintain performance and durability under high thermal stress.

3. MATERIAL AND METHOD

Disc brake system includes disc(rotor), caliper, pads, pistons and sealing elements. The pistons are driven by hydraulic oil in the caliper. Then, the pistons press against the pads, and the pads compress the disc to stop it. This is the general working theory of disc brake system.

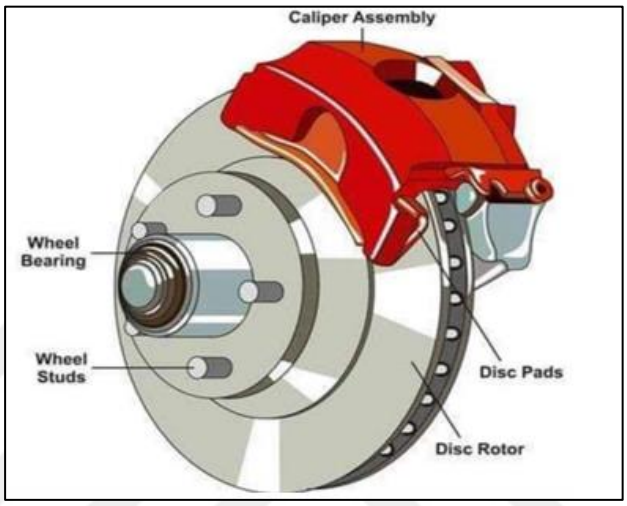

Figure 3.1. Example of disc brake system

The brake disc is mounted on the axle. The wheel is mounted on the axle. Brake pads are used as friction plates. Brake pads are located inside the brake caliper. By rubbing the brake disc on both surfaces through the pads, the brake disc is enabled to slow down or stop the wheel. In this working principle, the brake pads inside the brake caliper can be driven mechanically, hydraulically, pneumatically or electromagnetically.

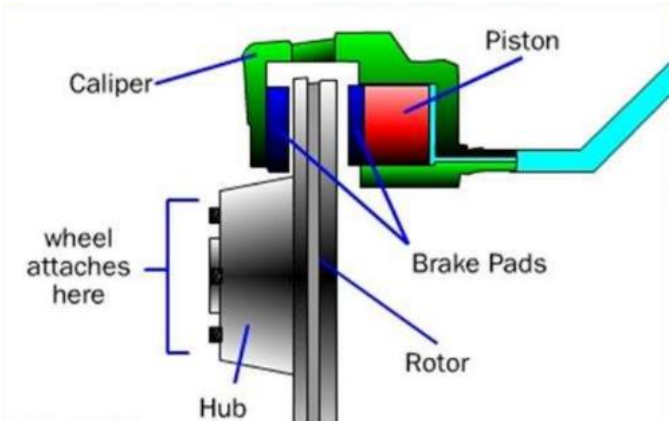

Figure 3.2. Components of disc brake system

3.1. Benchmarking of Disc Brake System

First, similar brake systems were examined, and their design parameters were compared. Benchmark details such as pressure capacity, pads contact area, piston and disc diameter are given in the examples below.

Table 3.1. Benchmarking of disc brake system

Design Parameters			
Brand	Mico	Mico	Brembo
Pressure Capacity(bar)	100	100	70
Pads Contact Area(mm^2)	10150	5045	3800
Piston Diameter(mm)	63.5	60	30
Disc Diameter(mm)	355	300	300

3.2. Conceptual Design of Disc Brake System

So, conceptual design was created based on benchmarking examples. First, a brake caliper containing brake pistons, brake pads and sealing elements is designed.

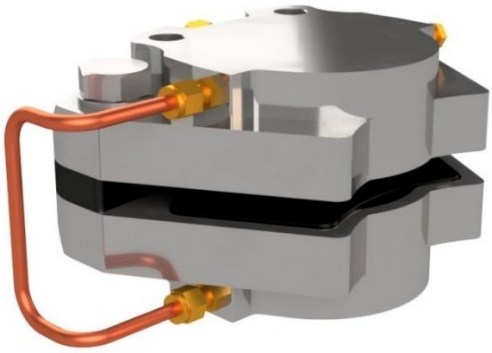

Figure 3.3. Conceptual design of brake caliper

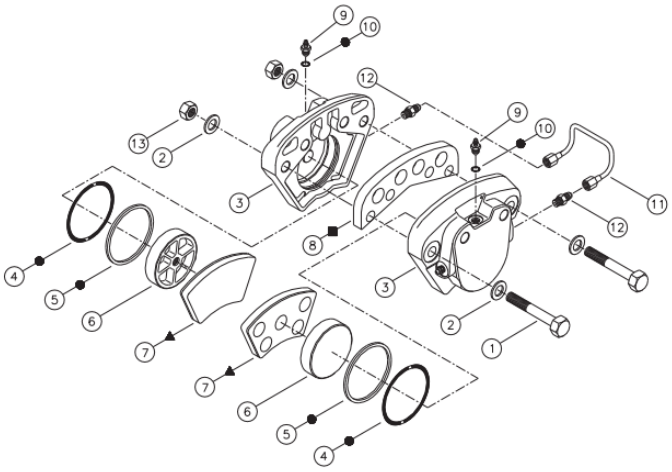

Figure 3.4. Exploded view of conceptual design

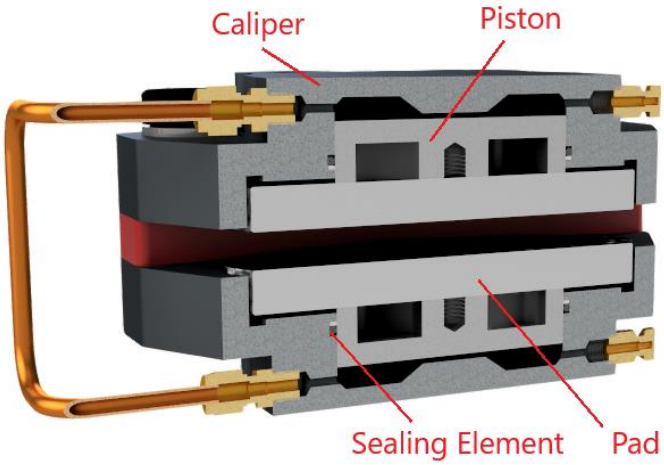

Figure 3.5. Details of conceptual design

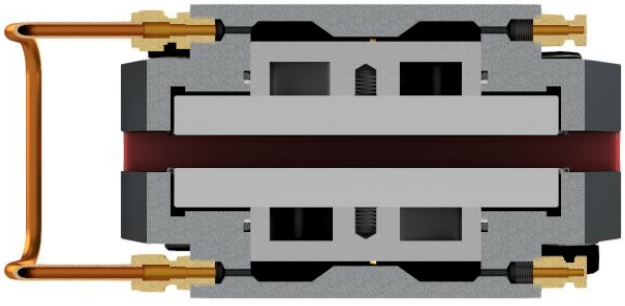

Figure 3.6. Section view of conceptual design

After, the brake disc was designed conceptually. The brake caliper and brake disc were assembled, and the packaging was checked.

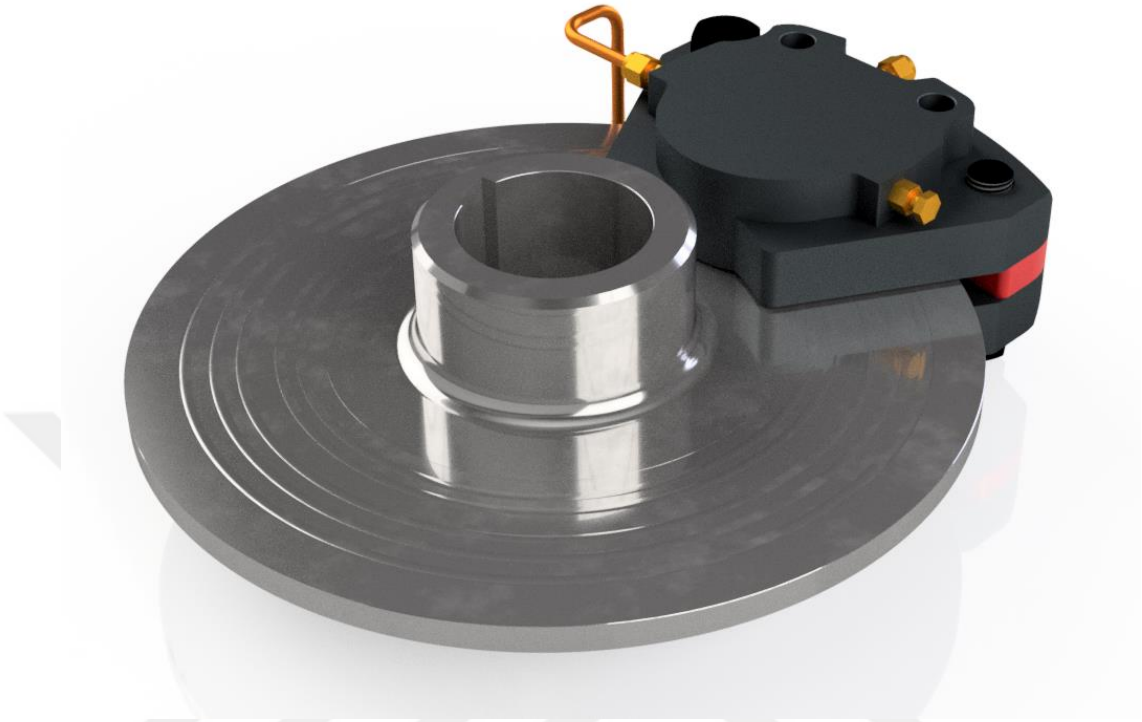

Figure 3.7. Brake disc and brake caliper assembly

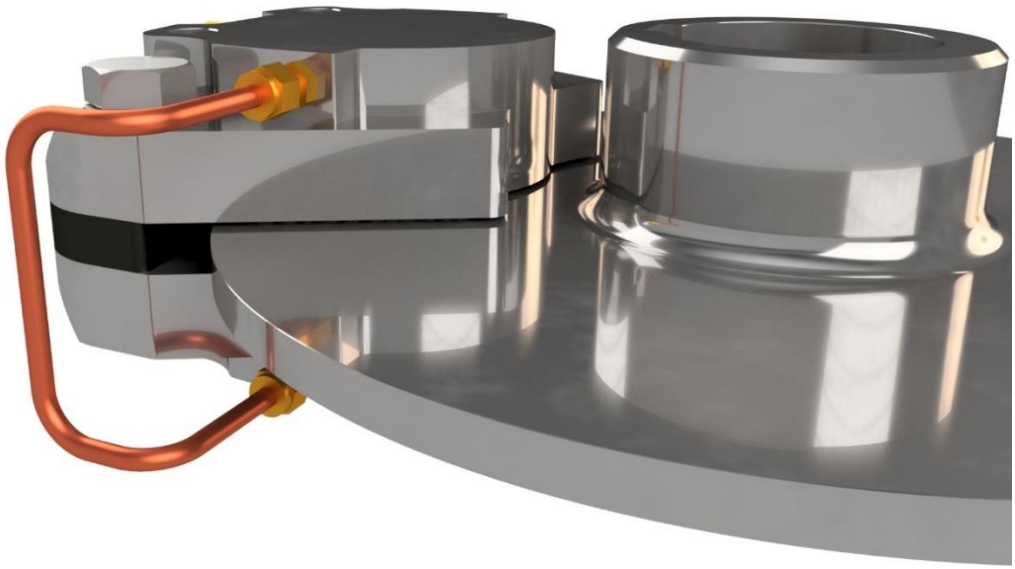

Figure 3.8. Brake disc and brake caliper packing control

3.3. Material Properties

Based on literature review, three different material qualities were determined as aluminum, stainless steel and structural steel for two different designs. First design geometry is a solid disc and second one is a ventilated disc. The table of analysis geometries and material qualities are given below:

Table 3.2. The table of analysis geometries and material qualities

Design Geometry	Material Quality
Solid	Aluminum Alloy
Solid	Stainless Steel
Solid	Structural Steel
Ventilated	Aluminum Alloy
Ventilated	Stainless Steel
Ventilated	Structural Steel

Carbon ceramic was determined for brake pads for all cases because it is commonly used.

Table 3.3. Material properties of brake pad

Properties	Carbon Ceramic	Units
Density	2040	kg/m^3
Elastic Modulus	2600	MPa
Poisson's Ratio	0.34	-
Bulk Modulus	2708.3	MPa
Shear Modulus	907.15	MPa
Tensile Yield Strength	250	MPa
Compressive Yield Strength	250	MPa
Tensile Ultimate Strength	460	MPa
Compressive Ultimate Strength	460	MPa
Coefficient of Thermal Expansion	0.000012	1/°C
Thermal Conductivity	8	W/mK
Specific Heat	1.123	J/gK

Table 3.4. Material properties of disc

Properties	Aluminum Alloy	Stainless Steel	Structural Steel	Units
Density	2770	7750	7850	kg/m^3
Elastic Modulus	70000	190000	210000	MPa
Poisson's Ratio	0.3897	0.29	0.28	-
Bulk Modulus	105770	150790	159090	MPa
Shear Modulus	25185	73643	82031	MPa
Tensile Yield Strength	45	207	275	MPa
Compressive Yield Strength	45	207	275	MPa
Tensile Ultimate Strength	110	517	450	MPa
Compressive Ultimate Strength	110	517	450	MPa
Coefficient of Thermal Expansion	0.000023	0.000017	0.000011	1/°C
Thermal Conductivity	171	36	14	W/mK
Specific Heat	875	500	440	J/gK

3.4. Calculations

The assumptions and input parameters made for the calculations are given below:

Table 3.5. Disc parameters

Specifications	Values	Units
Inner Diameter	100	mm
Outer Diameter (r)	200	mm
Thickness	5	mm

Table 3.6. Pad parameters

Specifications	Values	Units
Area (P_A)	450	mm^2
Thickness	5	mm

F. Talati and S. Jalalifar in their 2008 study and Limpert Rudolf in his study 1992, highlighted the input parameters, calculation assumptions and formulas as energy generated during braking, stopping distance, braking deceleration, deceleration time, braking power and heat flux.

Mr. Adarsh Bhat, Dr. Bhaskar Pal, Dr. Devendra Dandotiya in their 2024 study, explained the calculation assumptions and formulas such as braking force, braking torque and pad pressure.

Table 3.7. Input parameters

Specifications	Values	Units
Mass of the Vehicle (M)	1310	kg
Initial Velocity (u)	27.77	m/s
Last Velocity (v)	0	m/s
Axle Weight Distribution 50% on each side (γ)	0.5	-
Coefficient of Friction for Dry Pavement (μ)	0.7	-
Acceleration Due to Gravity (g)	9.81	m/s^2

- Calculation of Stopping Distance (s)

$$s = \frac{u^2}{2\mu g} = \mathbf{56.15\ m}$$

- Calculation of Braking Deceleration (a)

$$v^2 = u^2 + 2as \quad a = \mathbf{6.86\ m/s^2}$$

- Calculation of Braking Force (F_b)

$$F_b = \gamma * M * a = \mathbf{4500\ N}$$

- Calculation of Pad Pressure (P_p)

$$P_p = \frac{F_b}{P_A} = \mathbf{10\ MPa}$$

- Calculation Deceleration Time (B_t)

$$v = u + at \quad B_t = \mathbf{4\ s}$$

3.5. Finite Element Analysis

The steps of finite element analysis are geometry, meshing, boundary conditions and results.

- **Geometry**

  Two analysis geometries which are solid and ventilated were designed with the Solidworks program according to the dimensions specified in tables 3.5. and 3.6.

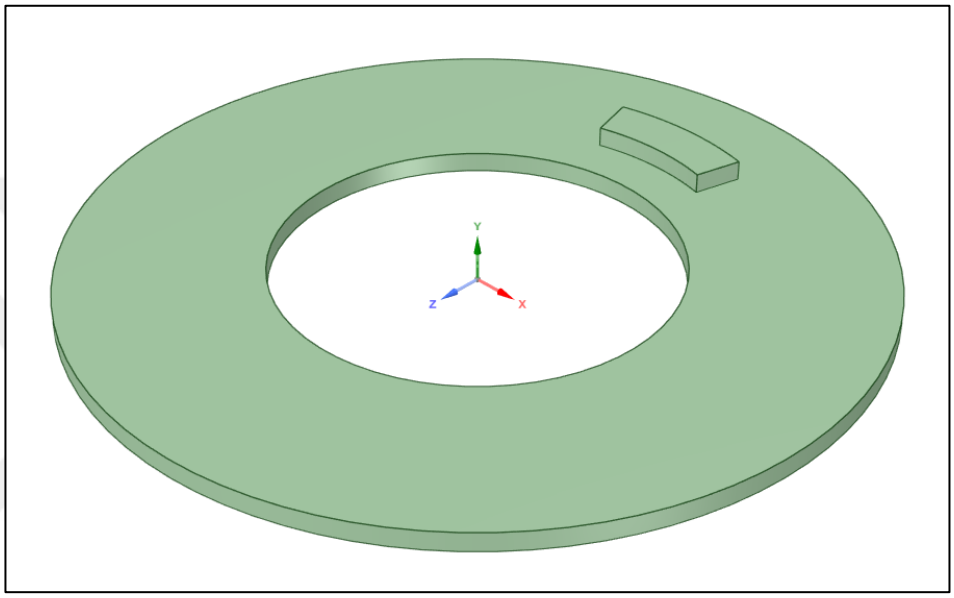

Figure 3.9. Solid disc brake model

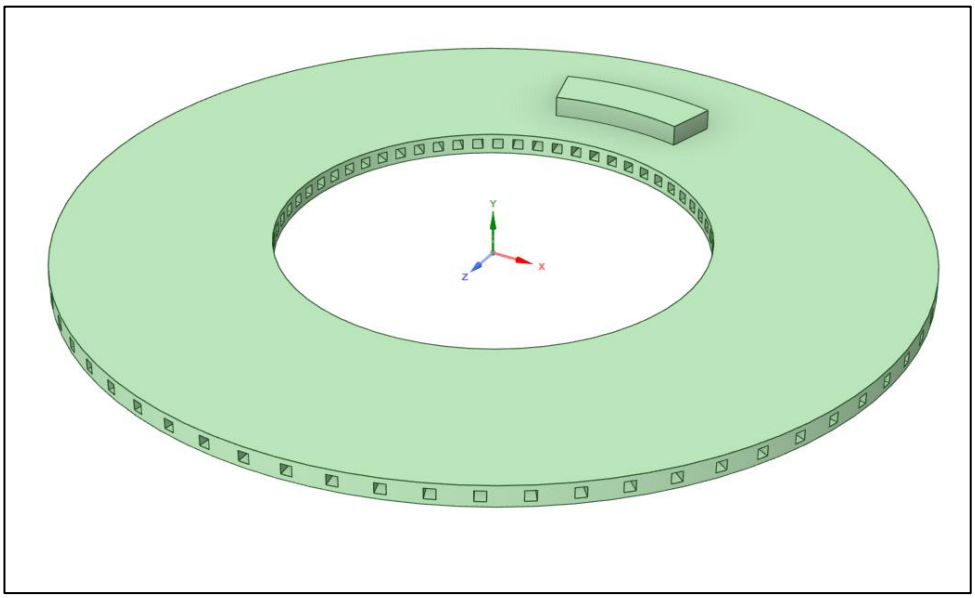

Figure 3.10. Ventilated disc brake model

- **Analysis Cases**

The two geometrical models were imported to ANSYS, eighteen cases and three different material properties were assigned as shown below.

Table 3.8. Analysis cases

Analysis Method	Cases	Geometry	Material Quality	Braking Pressure
STRUCTURAL ANALYSIS	**Case-1**	Solid	Structural Steel	10 MPa
	Case-2	Solid	Stainless Steel	10 MPa
	Case-3	Solid	Aluminum Alloy	10 MPa
	Case-4	Ventilated	Structural Steel	10 MPa
	Case-5	Ventilated	Stainless Steel	10 MPa
	Case-6	Ventilated	Aluminum Alloy	10 MPa
	Case-7	Solid	Structural Steel	20 MPa
	Case-8	Solid	Stainless Steel	20 MPa
	Case-9	Solid	Aluminum Alloy	20 MPa
	Case-10	Ventilated	Structural Steel	20 MPa
	Case-11	Ventilated	Stainless Steel	20 MPa
	Case-12	Ventilated	Aluminum Alloy	20 MPa
THERMAL & STRUCTURAL ANALYSIS (COUPLED)	**Case-13**	Solid	Structural Steel	10 MPa
	Case-14	Solid	Stainless Steel	10 MPa
	Case-15	Solid	Aluminum Alloy	10 MPa
	Case-16	Ventilated	Structural Steel	10 MPa
	Case-17	Ventilated	Stainless Steel	10 MPa
	Case-18	Ventilated	Aluminum Alloy	10 MPa

- Meshing

Meshing stage is very important in finite element analysis in terms of numerical convergence. The more the mesh quality is increased, the more accurate results are achieved. In this study, fine meshing was done hexagonal surface mesher with a minimum element size of 5 mm for solid disc brake and minimum element size of 2.5 mm for ventilated disc brake. Mesh models generated are shown figure 3.11. and 3.12.

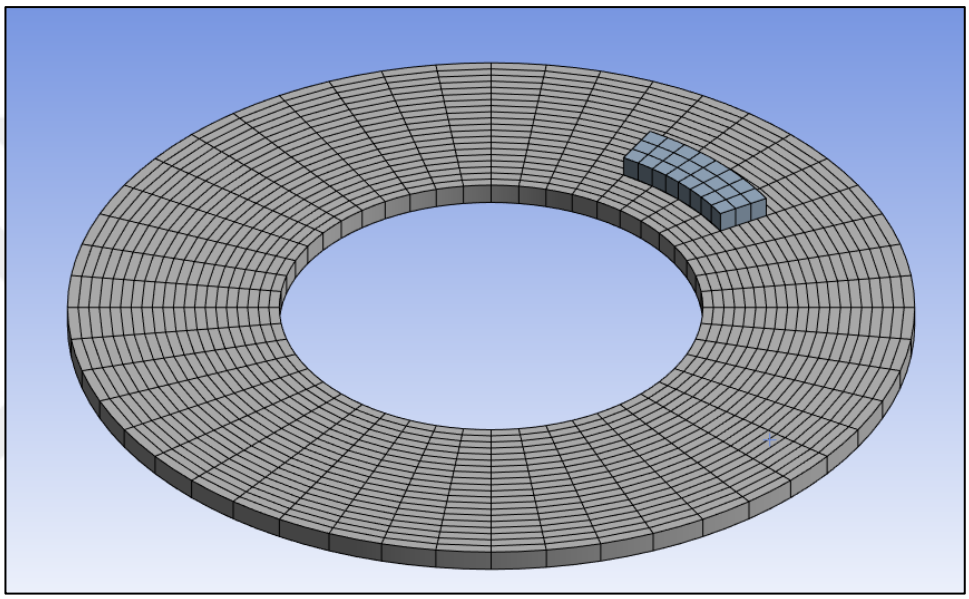

Figure 3.11. Solid disc brake meshing

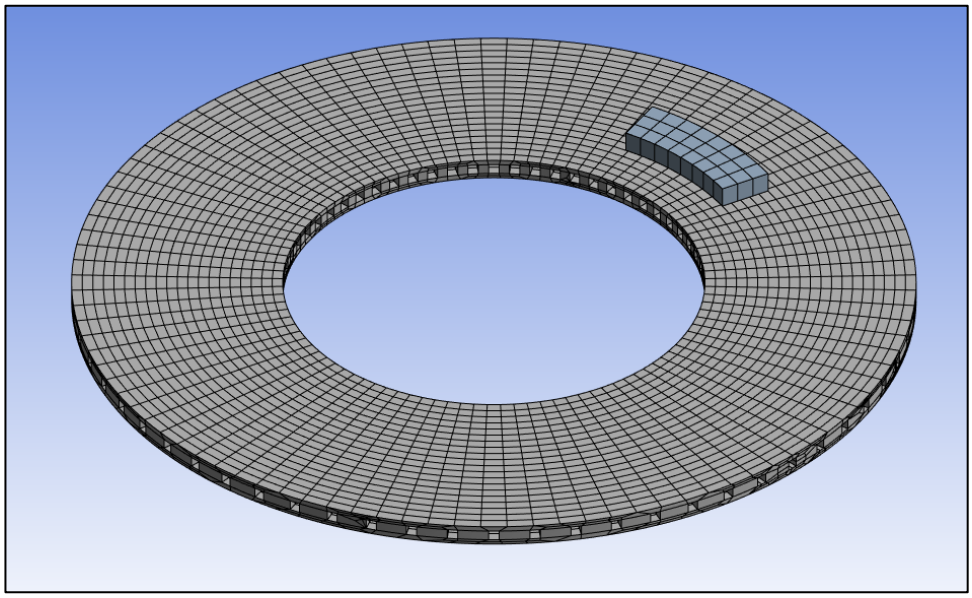

Figure 3.12. Ventilated disc brake meshing

- **Boundary Conditions**

  Boundary conditions are the same from case-1 to case-12 for structural analysis method according to table 3.8. Geometry, material quality and braking pressure have been changed.

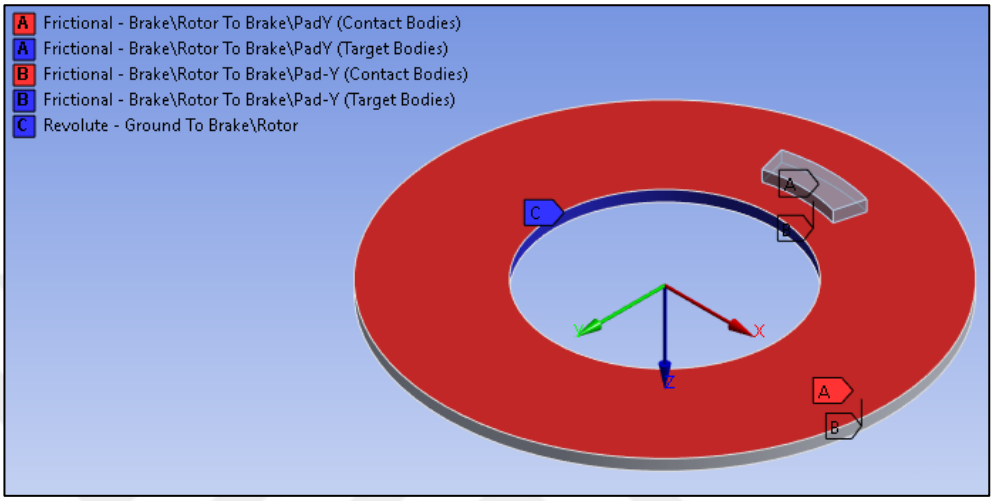

Figure 3.13. Boundary conditions of solid disc for structural analysis method

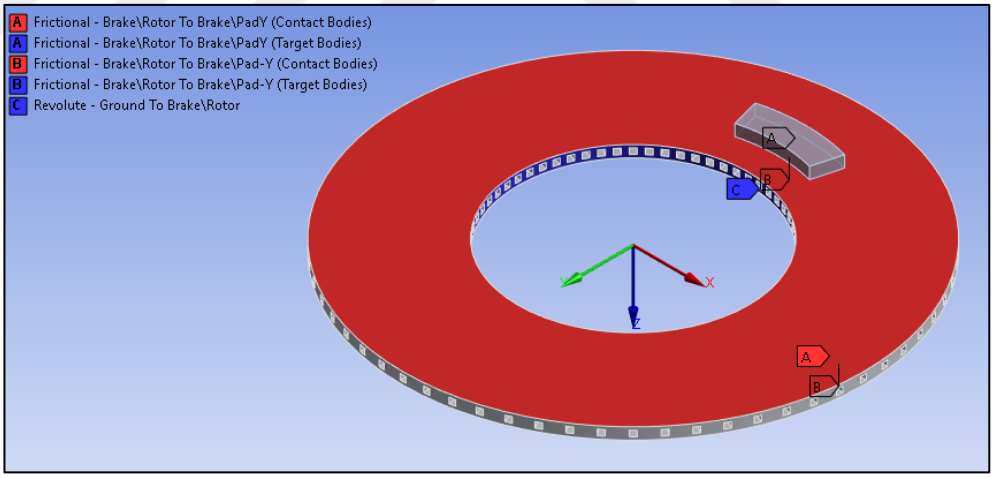

Figure 3.14. Boundary conditions of ventilated brake for structural analysis method

10 MPa brake pressure was applied from case-1 to case-6 for solid and ventilated disc brake. Also, rotational velocity and pressure are processed as tabular data.

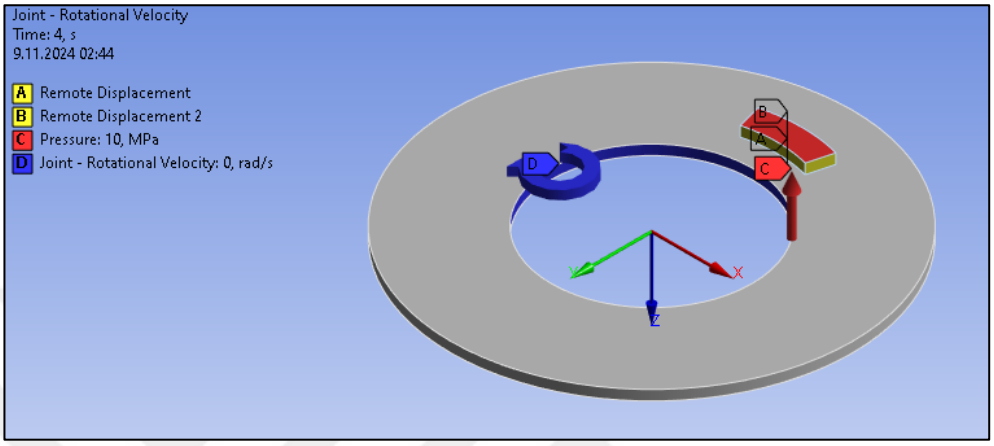

Figure 3.15. Analysis settings of solid disc for structural analysis method

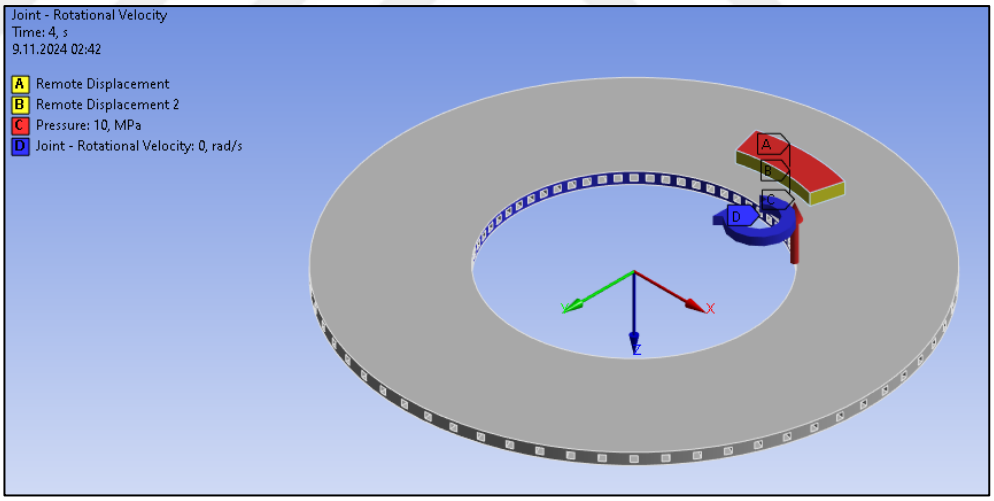

Figure 3.16. Analysis settings of ventilated disc for structural analysis method

20 MPa brake pressure was applied from case-7 to case-12 for solid and ventilated disc brake. Also, rotational velocity and pressure are processed as tabular data.

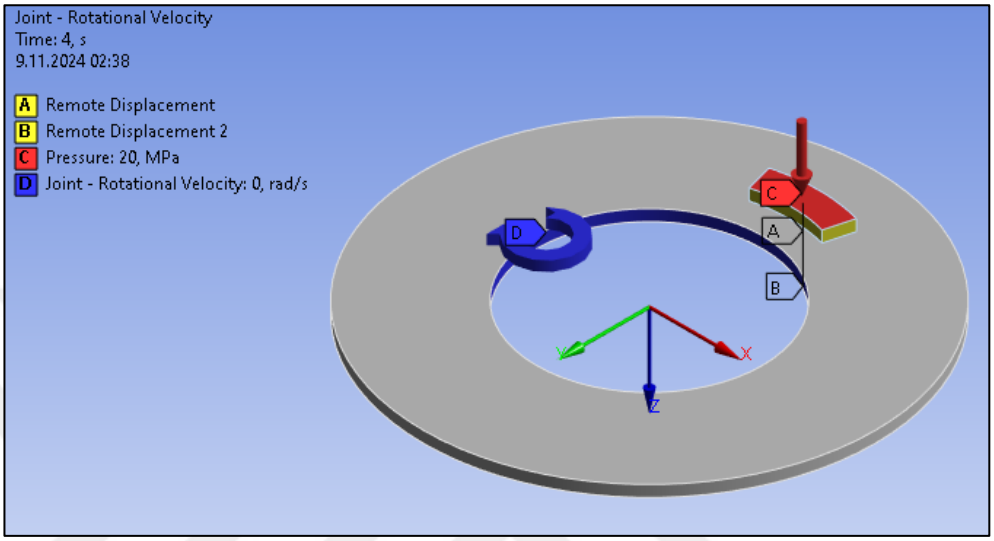

Figure 3.17. Analysis settings of solid disc for structural analysis method

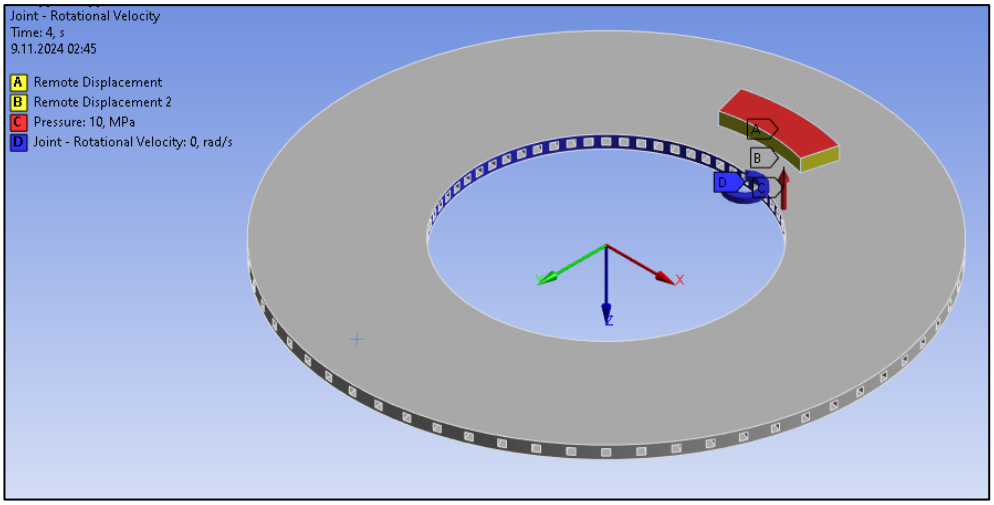

Figure 3.18. Analysis settings of ventilated disc for structural analysis method

Boundary conditions are the same from case-13 to case-18 for thermal and structural analysis method (coupled) according to table 3.8. Geometry, material quality and braking pressure have been changed.

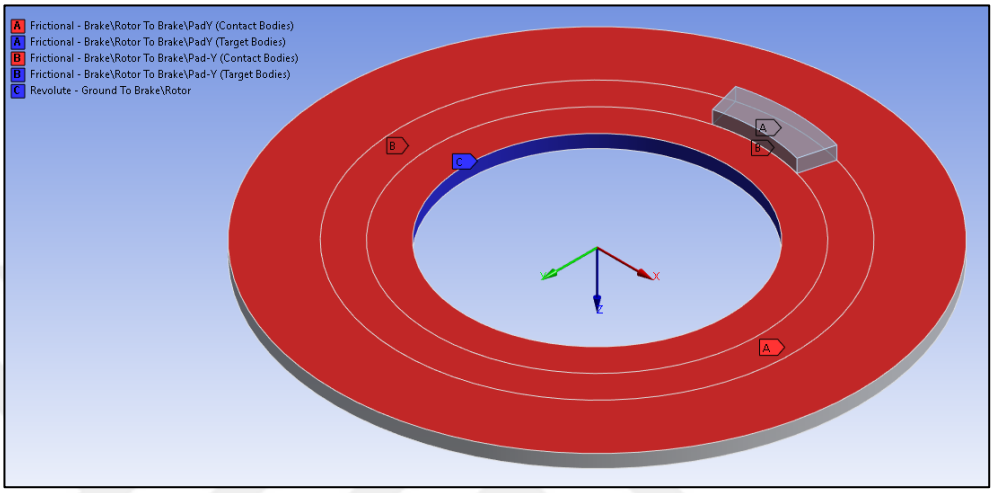

Figure 3.19. Boundary conditions of solid disc for coupled analysis method

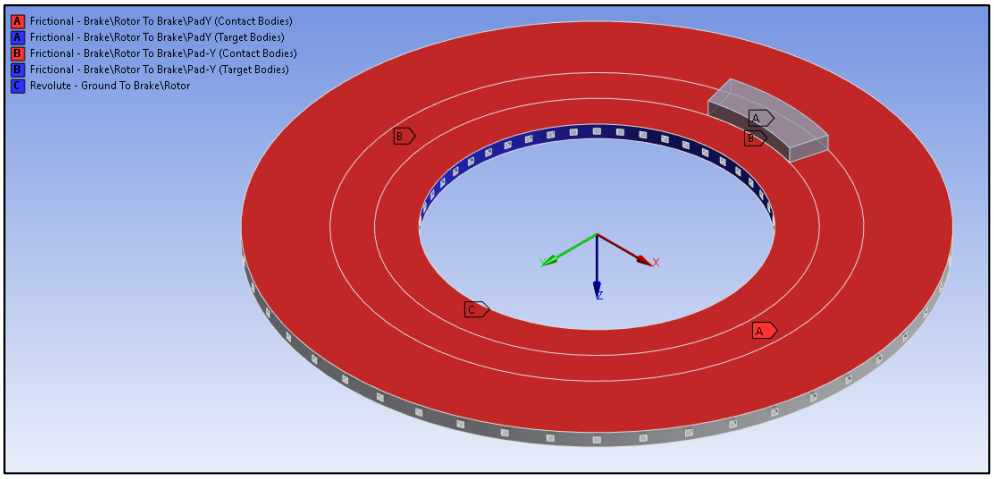

Figure 3.20. Boundary conditions of ventilated disc for coupled analysis method

10 MPa brake pressure, 100 °C constant temperature and 0.01 constant film coefficient for convection were applied from case-13 to case-18 for solid and ventilated disc brake. Also, rotational velocity and pressure are processed as tabular data.

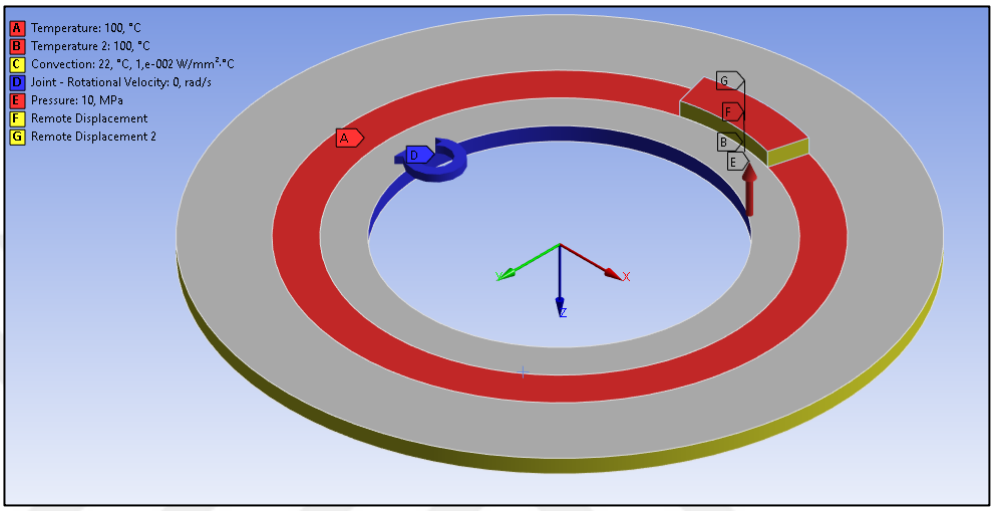

Figure 3.21. Analysis settings of solid disc for coupled analysis method

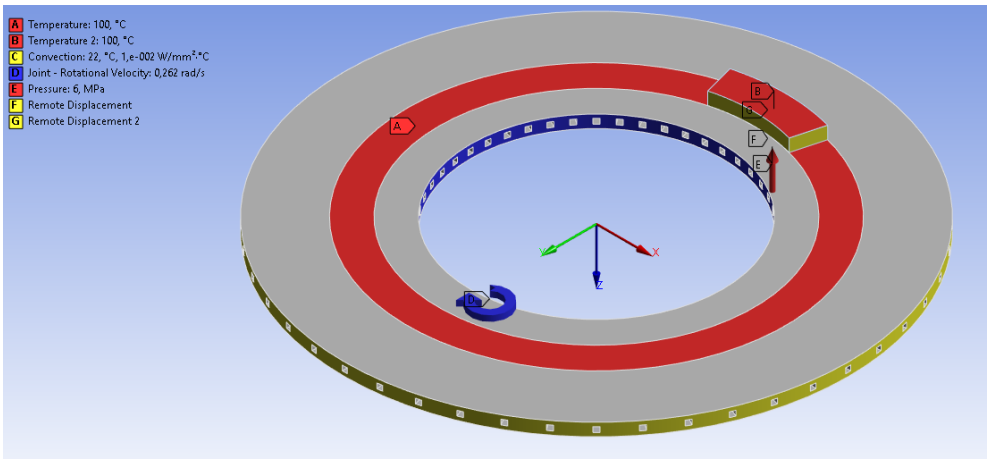

Figure 3.22. Analysis settings of ventilated disc for coupled analysis method

4. RESULTS

Eighteen analysis cases were run according to boundary conditions, analysis inputs and table 3.8. Equivalent stress, total deformation, equivalent elastic strain were evaluated.

Analysis results of case-1;

Equivalent stress is 24.263 MPa according to the analysis result.

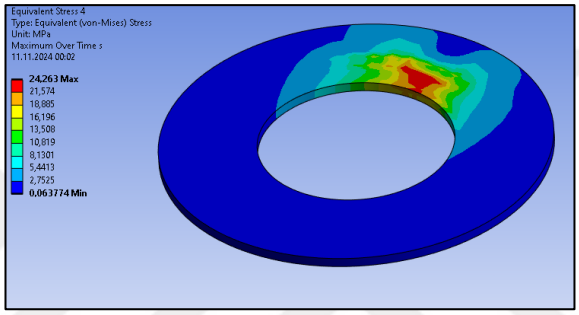

Figure 4.1. Equivalent stress for case-1

Total deformation is 85.662 mm according to the analysis result.

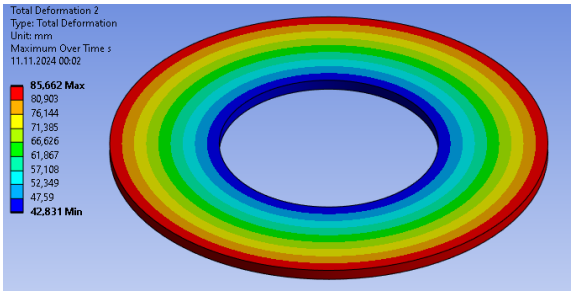

Figure 4.2. Total deformation for case-1

Directional deformation of X axis is 85.65 mm according to the analysis result.

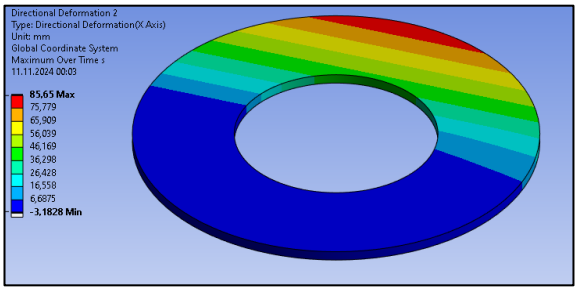

Figure 4.3. Directional deformation of X axis for case-1

Directional deformation of Z axis is 85.651 mm according to the analysis result.

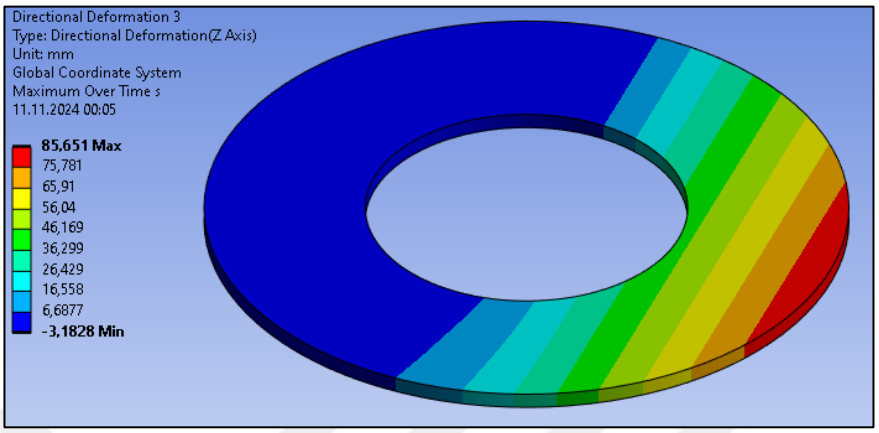

Figure 4.4. Directional deformation of Z axis for case-1

Directional deformation of Y axis is 0.0070521 mm according to the analysis result.

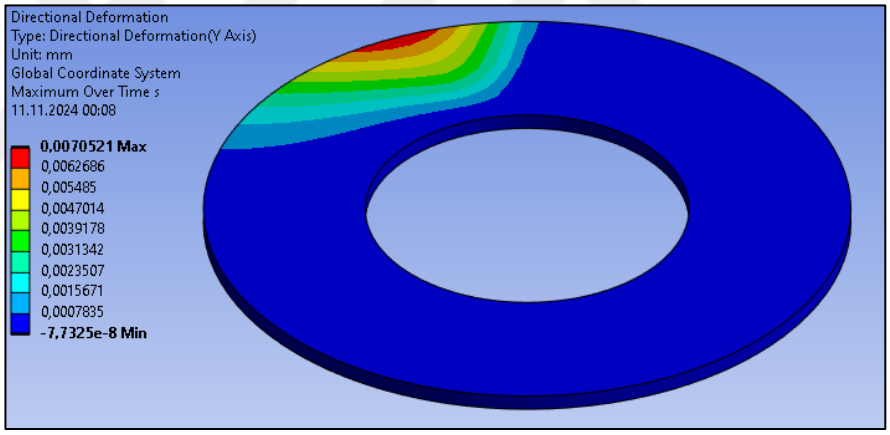

Figure 4.5. Directional deformation of Y axis for case-1

Equivalent elastic strain is 0.00011588 according to the analysis result.

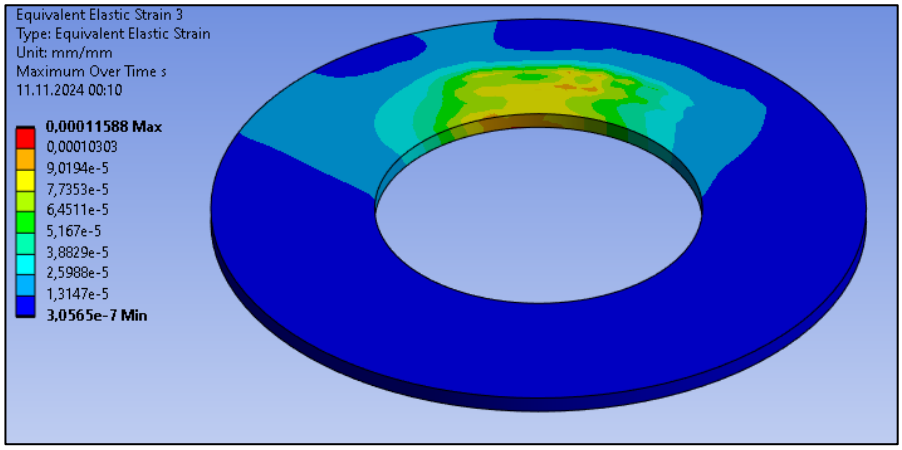

Figure 4.6. Equivalent elastic strain for case-1

Analysis results of case-2;

Equivalent stress is 24.022 MPa according to the analysis result.

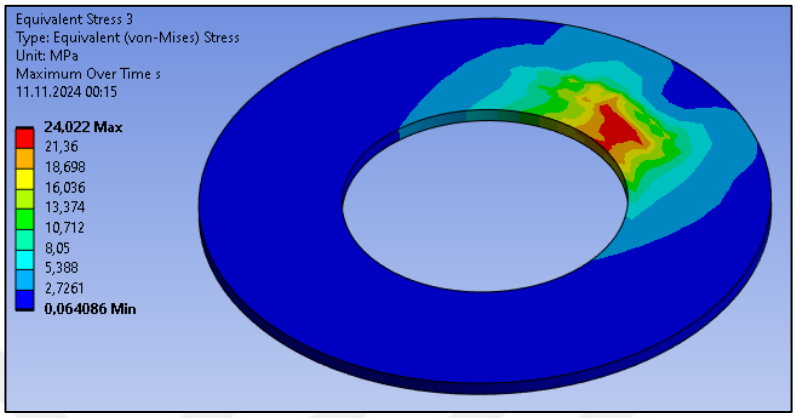

Figure 4.7. Equivalent stress for case-2

Total deformation is 85.662 mm according to the analysis result.

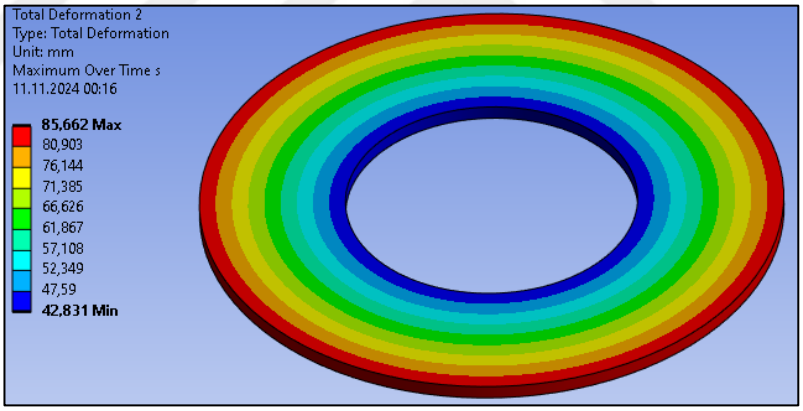

Figure 4.8. Total deformation for case-2

Directional deformation of X axis is 85.65 mm according to the analysis result.

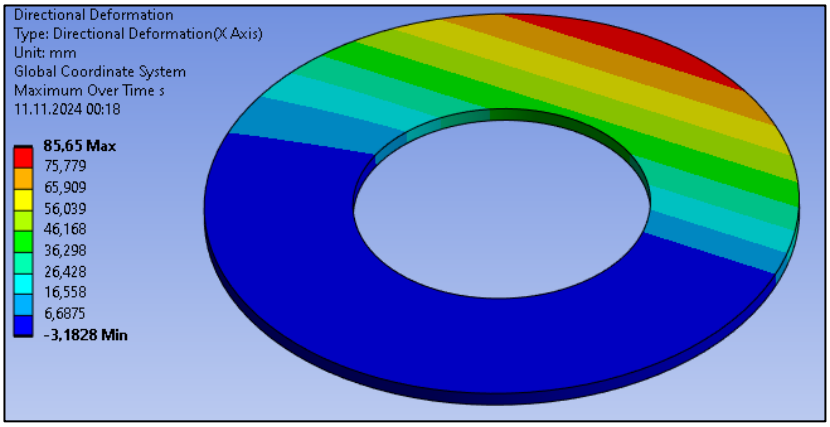

Figure 4.9. Directional deformation of X axis for case-2

Directional deformation of Z axis is 85.651 mm according to the analysis result.

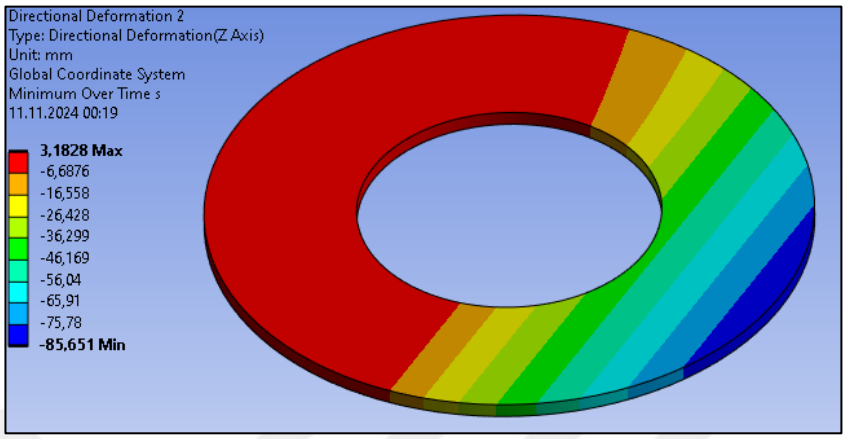

Figure 4.10. Directional deformation of Z axis for case-2

Directional deformation of Y axis is 0.0076362 mm according to the analysis result.

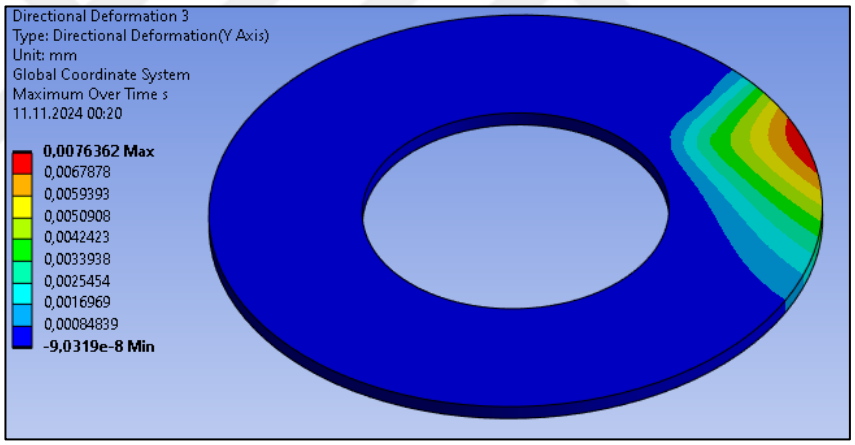

Figure 4.11. Directional deformation of Y axis for case-2

Equivalent elastic strain is 0.00012681 according to the analysis result.

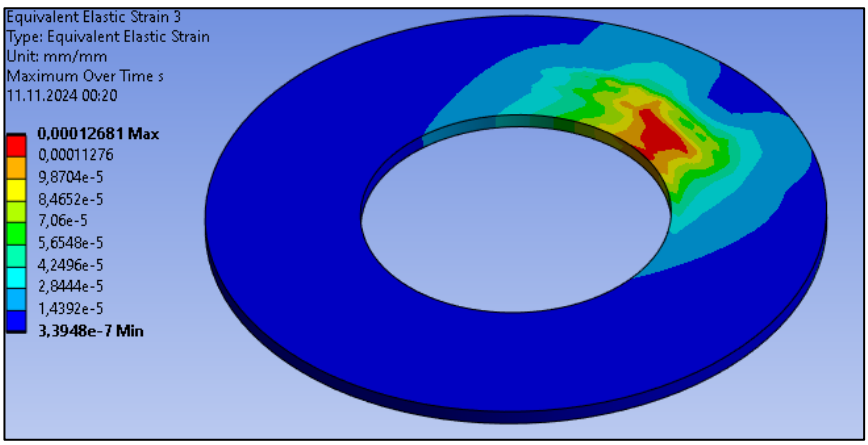

Figure 4.12. Equivalent elastic strain for case-2

Analysis results of case-3;

Equivalent stress is 21.641 MPa according to the analysis result.

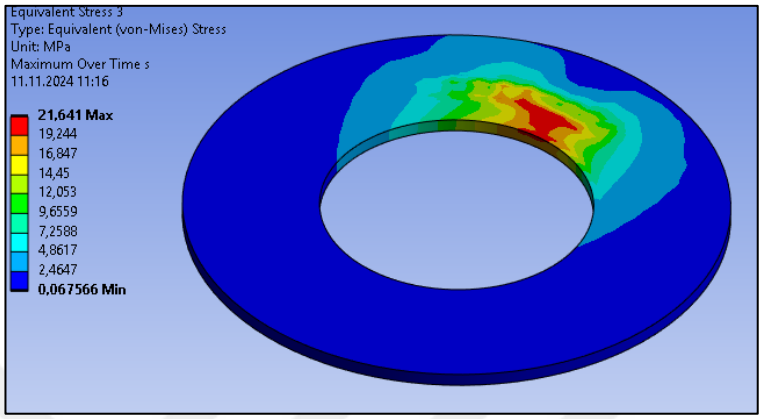

Figure 4.13. Equivalent stress for case-3

Total deformation is 85.661 mm according to the analysis result.

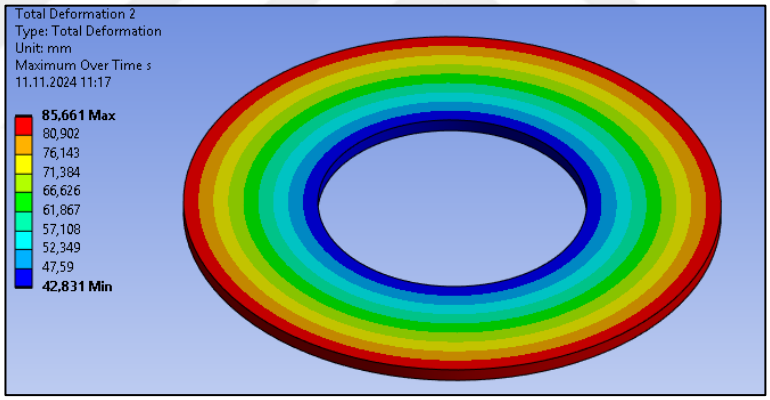

Figure 4.14. Total deformation for case-3

Directional deformation of X axis is 85.646 mm according to the analysis result.

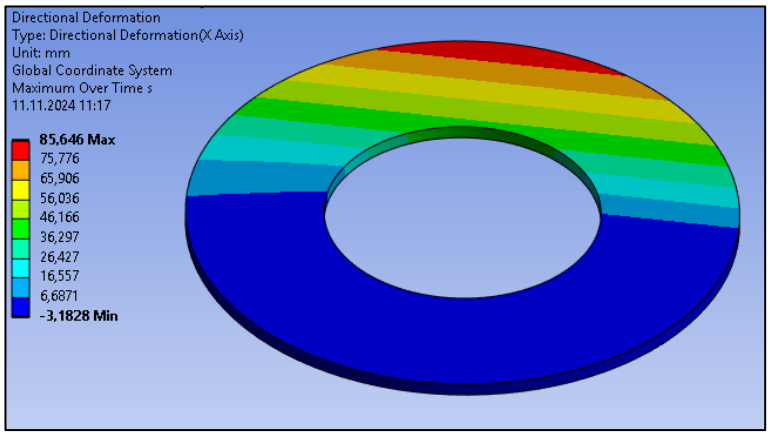

Figure 4.15. Directional deformation of X axis for case-3

Directional deformation of Z axis is 85.65 mm according to the analysis result.

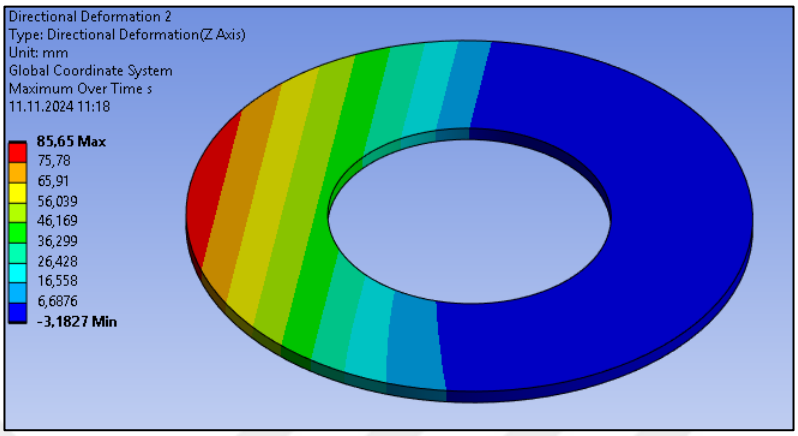

Figure 4.16. Directional deformation of Z axis for case-3

Directional deformation of Y axis is 0.015291 mm according to the analysis result.

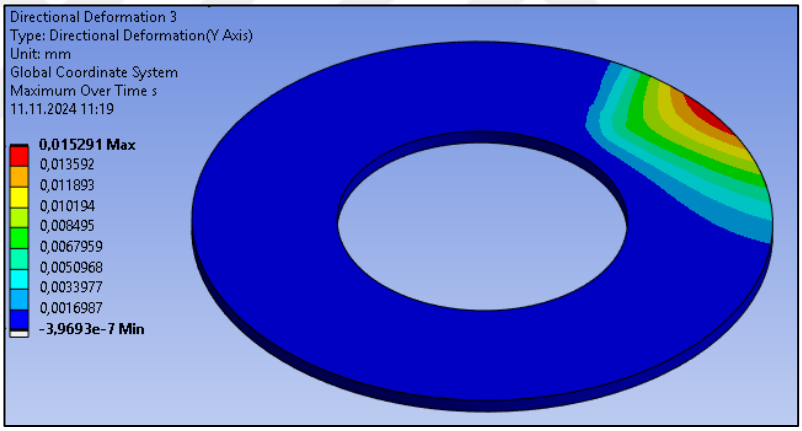

Figure 4.17. Directional deformation of Y axis for case-3

Equivalent elastic strain is 0.00031096 according to the analysis result.

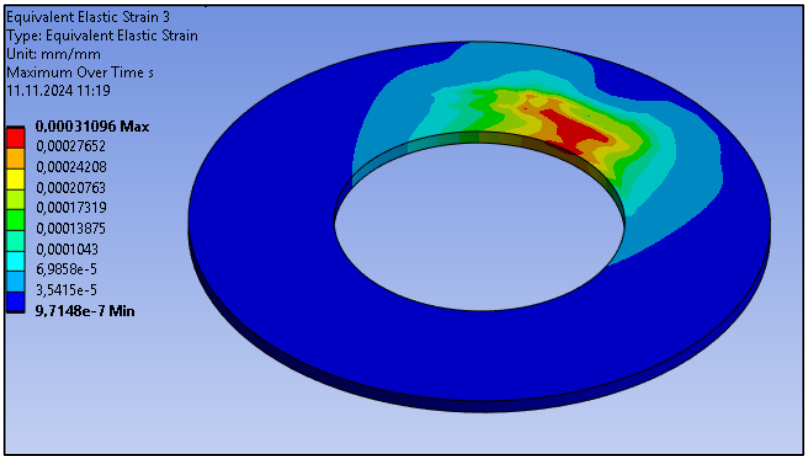

Figure 4.18. Equivalent elastic strain for case-3

Analysis results of case-4;

Equivalent stress is 37.613 MPa according to the analysis result.

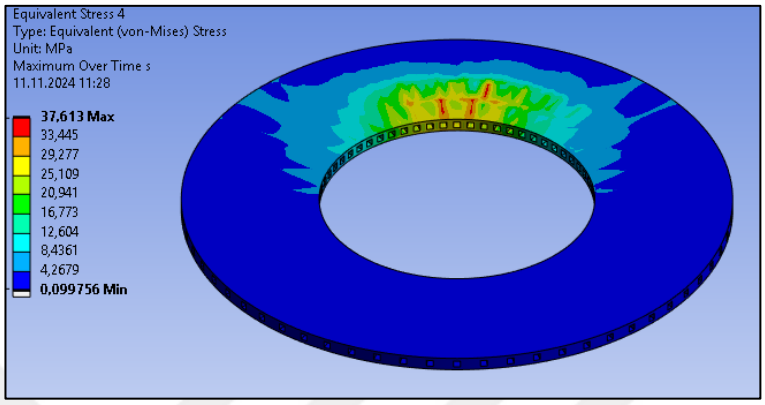

Figure 4.19. Equivalent stress for case-4

Total deformation is 85.662 mm according to the analysis result.

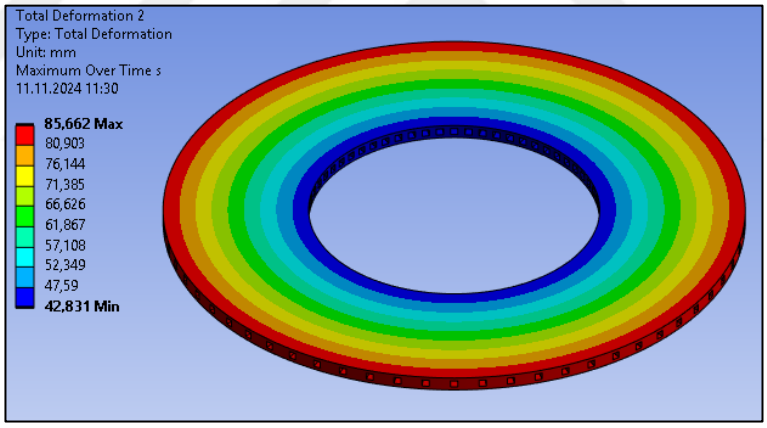

Figure 4.20. Total deformation for case-4

Directional deformation of X axis is 85.659 mm according to the analysis result.

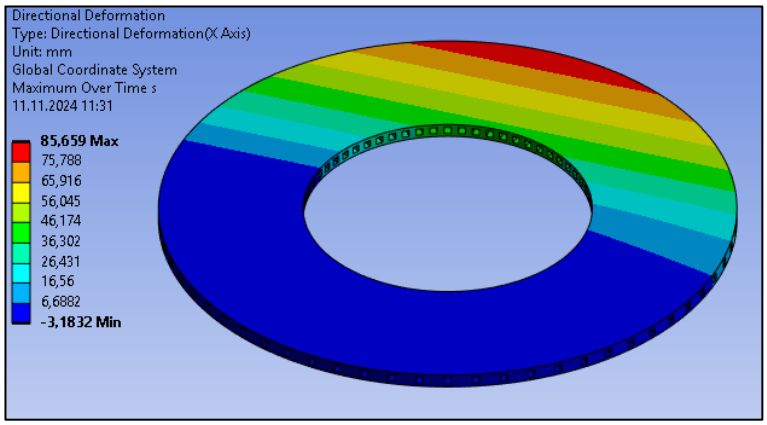

Figure 4.21. Directional deformation of X axis for case-4

Directional deformation of Z axis is 85.661 mm according to the analysis result.

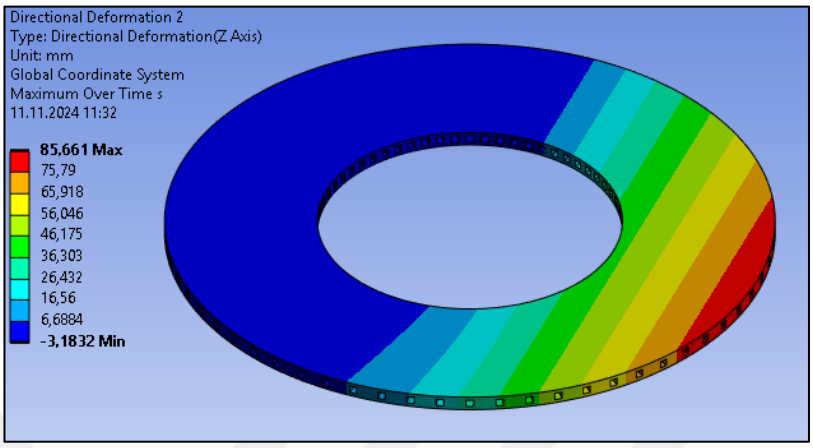

Figure 4.22. Directional deformation of Z axis for case-4

Directional deformation of Y axis is 0.0027779 mm according to the analysis result.

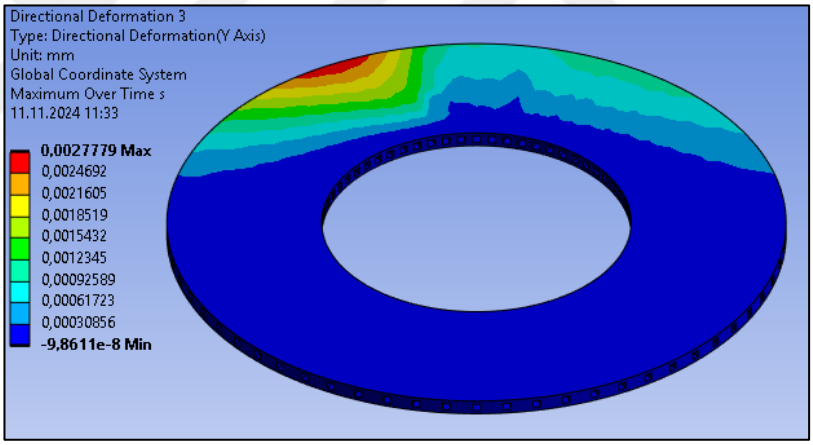

Figure 4.23. Directional deformation of Y axis for case-4

Equivalent elastic strain is 0.00018782 according to the analysis result.

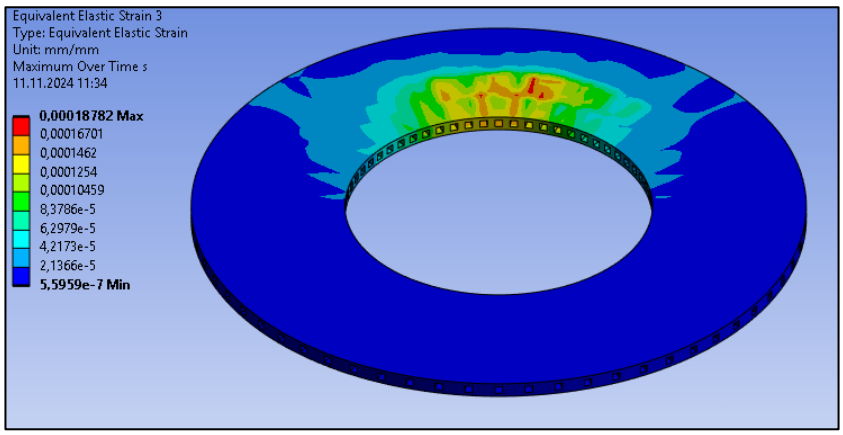

Figure 4.24. Equivalent elastic strain for case-4

Analysis results of case-5;

Equivalent stress is 36.881 MPa according to the analysis result.

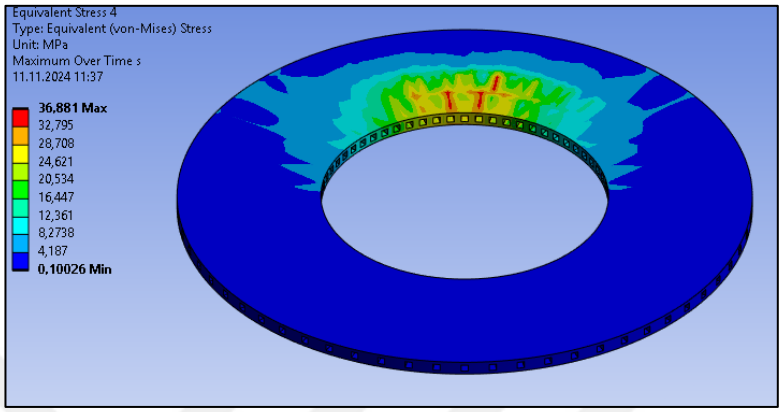

Figure 4.25. Equivalent stress for case-5

Total deformation is 85.662 mm according to the analysis result.

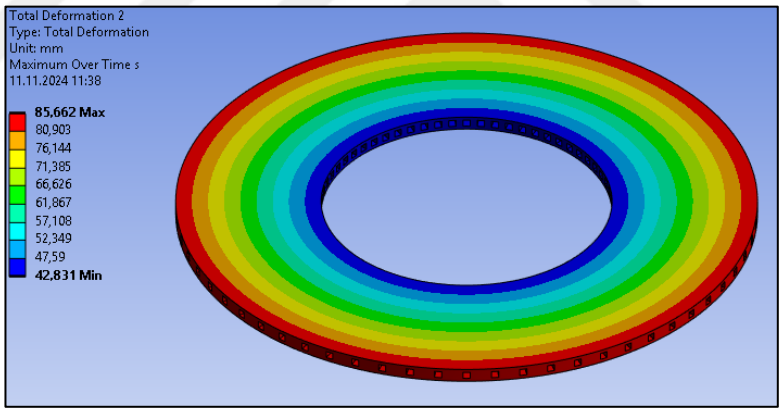

Figure 4.26. Total deformation for case-5

Directional deformation of X axis is 85.659 mm according to the analysis result.

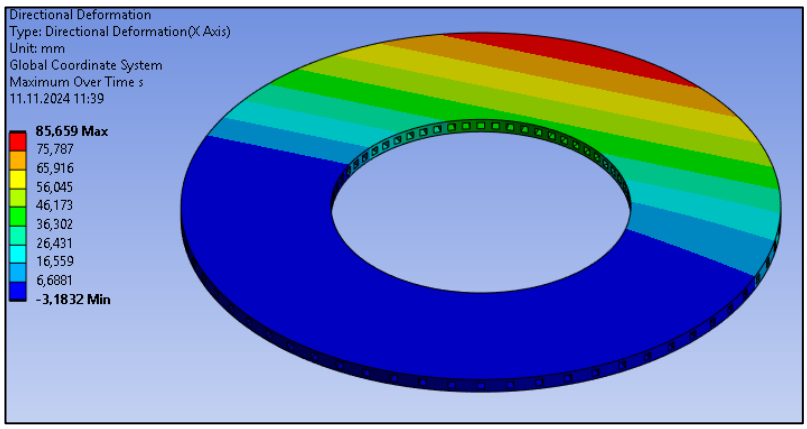

Figure 4.27. Directional deformation of X axis for case-5

Directional deformation of Z axis is 85.661 mm according to the analysis result.

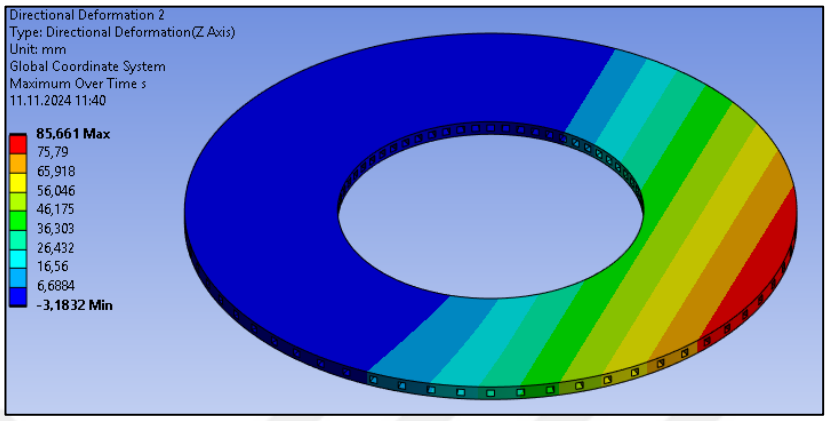

Figure 4.28. Directional deformation of Z axis for case-5

Directional deformation of Y axis is 0.0029053 mm according to the analysis result.

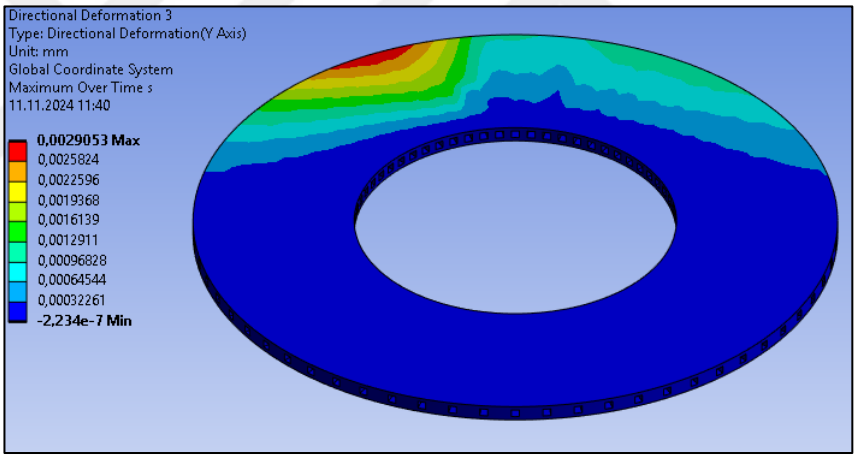

Figure 4.29. Directional deformation of Y axis for case-5

Equivalent elastic strain is 0.0002062 according to the analysis result.

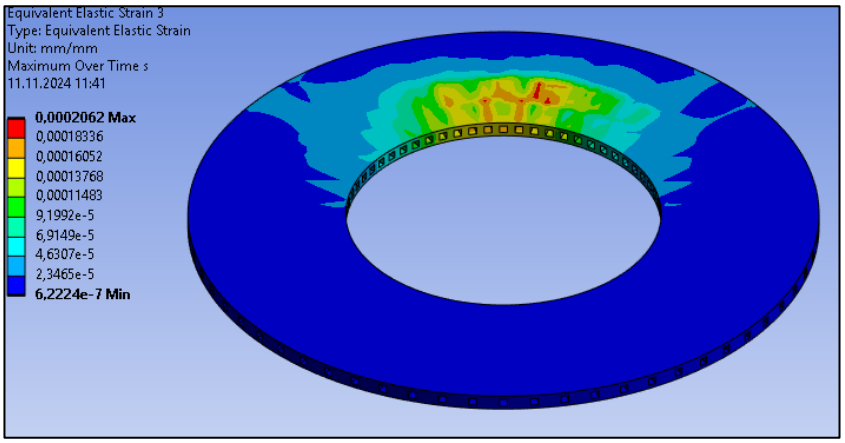

Figure 4.30. Equivalent elastic strain for case-5

Analysis results of case-6;

Equivalent stress is 34.939 MPa according to the analysis result.

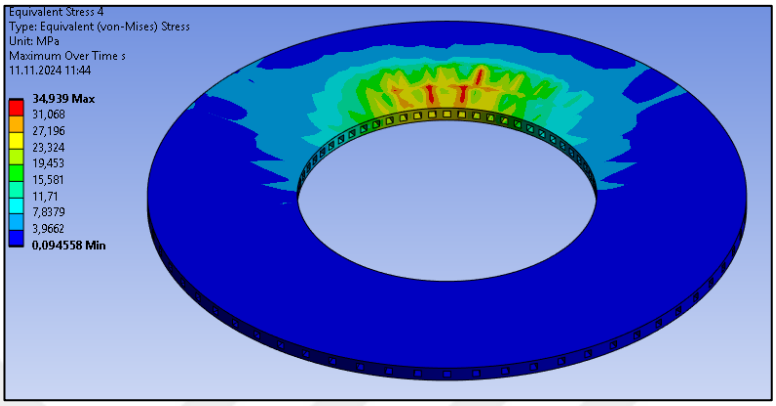

Figure 4.31. Equivalent stress for case-6

Total deformation is 85.661 mm according to the analysis result.

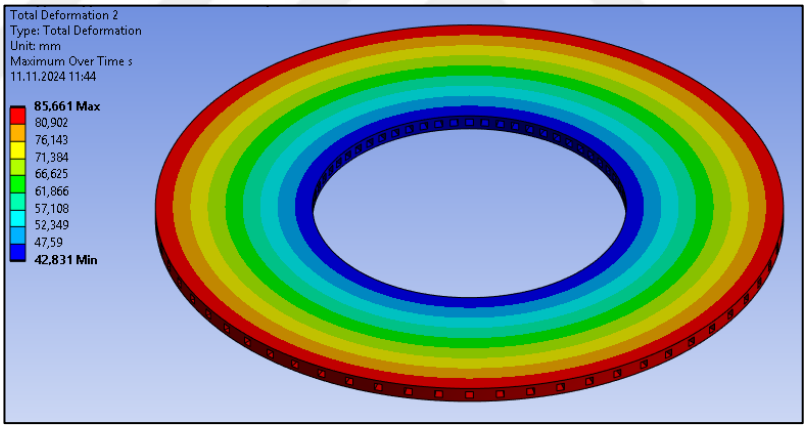

Figure 4.32. Total deformation for case-6

Directional deformation of X axis is 85.653 mm according to the analysis result.

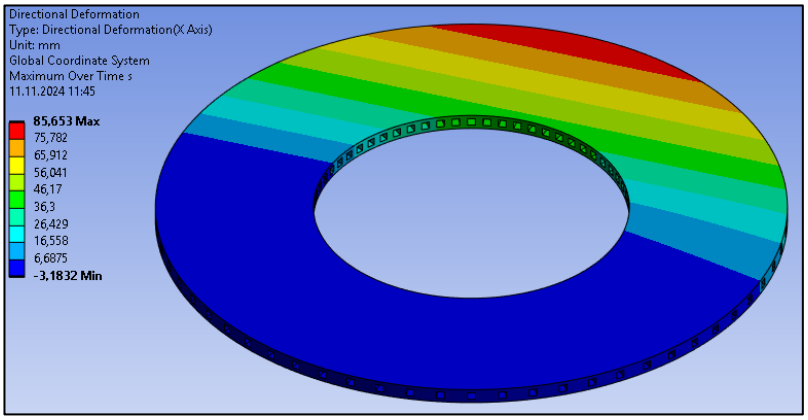

Figure 4.33. Directional deformation of X axis for case-6

Directional deformation of Z axis is 85.66 mm according to the analysis result.

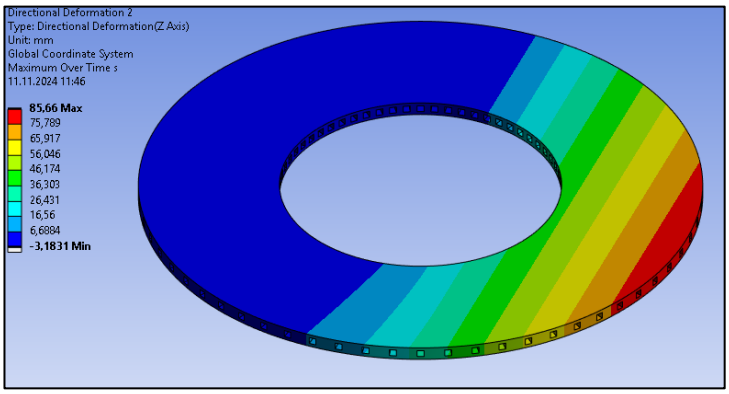

Figure 4.34. Directional deformation of Z axis for case-6

Directional deformation of Y axis is 0.0055514 mm according to the analysis result.

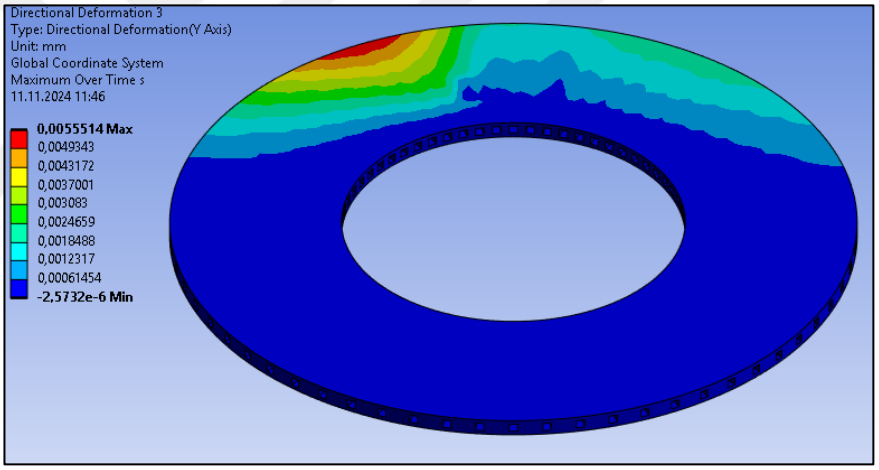

Figure 4.35. Directional deformation of Y axis for case-6

Equivalent elastic strain is 0.00052502 according to the analysis result.

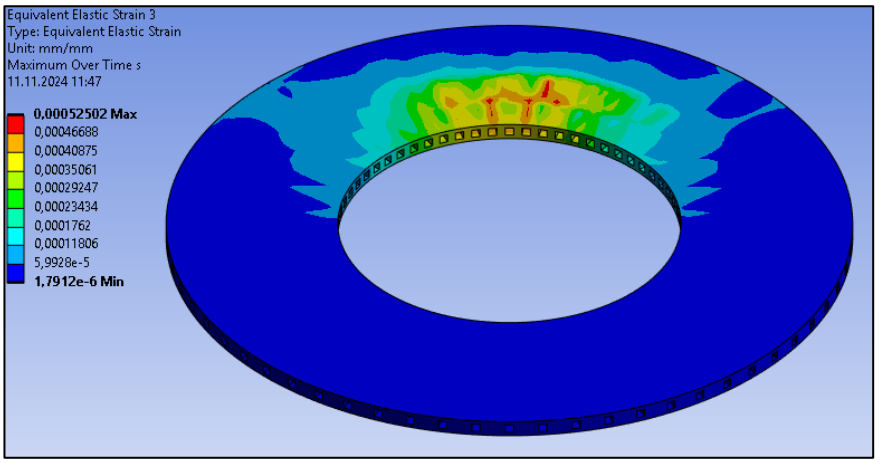

Figure 4.36. Equivalent elastic strain for case-6

Analysis results of case-7;

Equivalent stress is 40.615 MPa according to the analysis result.

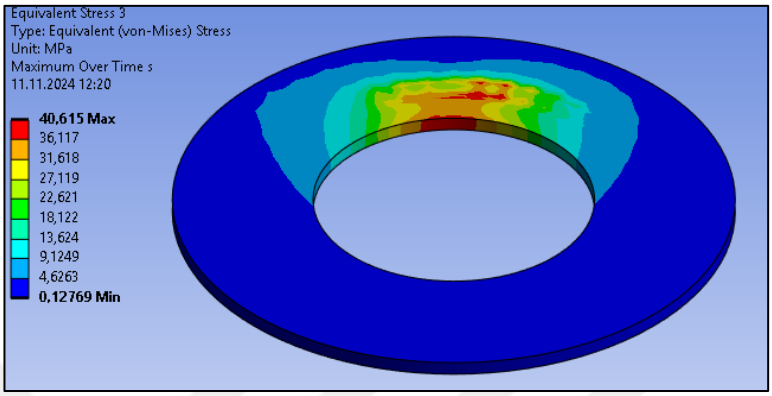

Figure 4.37. Equivalent stress for case-7

Total deformation is 85.662 mm according to the analysis result.

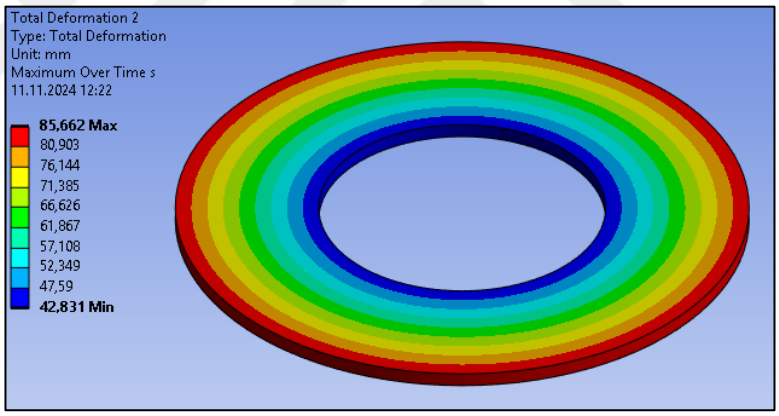

Figure 4.38. Total deformation for case-7

Directional deformation of X axis is 85.648 mm according to the analysis result.

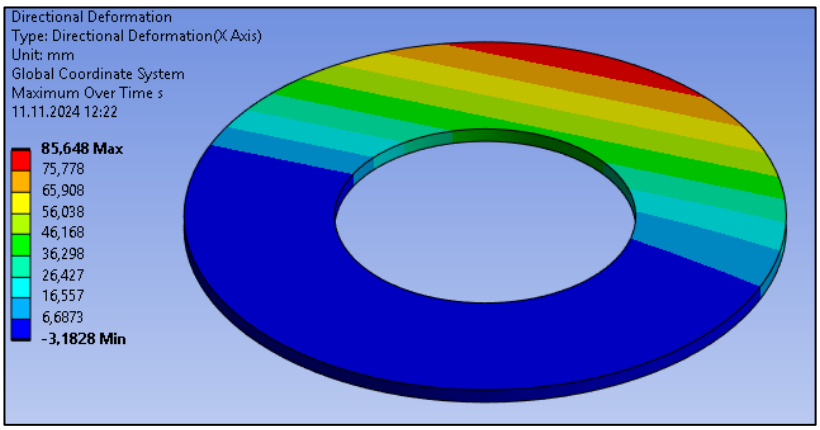

Figure 4.39. Directional deformation of X axis for case-7

Directional deformation of Z axis is 85.651 mm according to the analysis result.

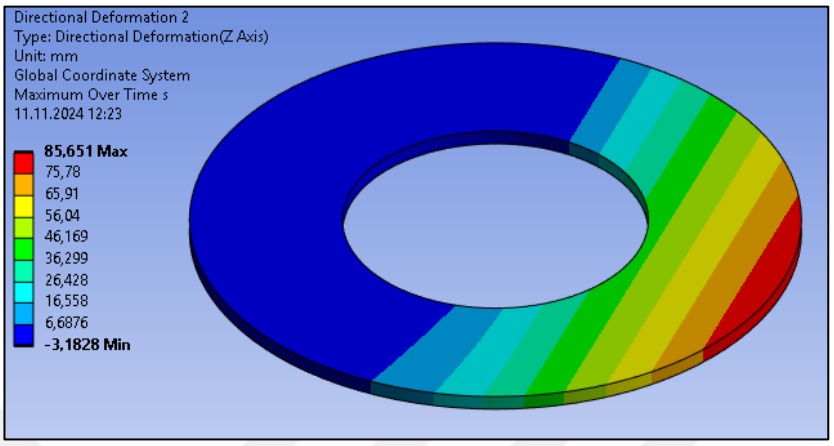

Figure 4.40. Directional deformation of Z axis for case-7

Directional deformation of Y axis is 0.0013977 mm according to the analysis result.

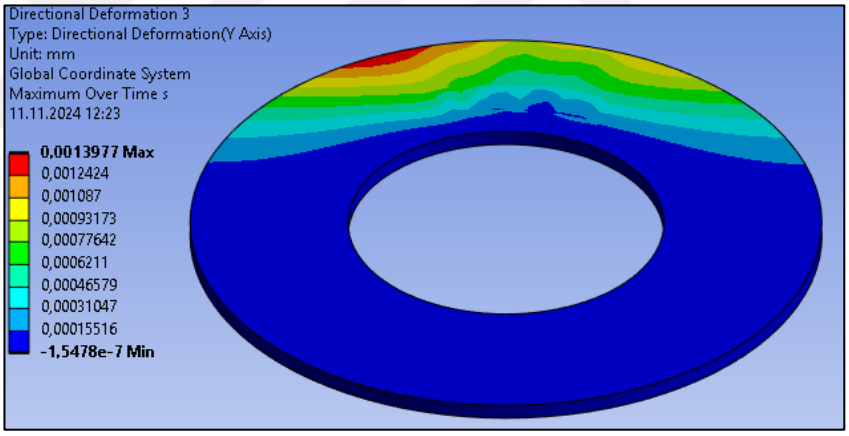

Figure 4.41. Directional deformation of Z axis for case-7

Equivalent elastic strain is 0.00019597 according to the analysis result.

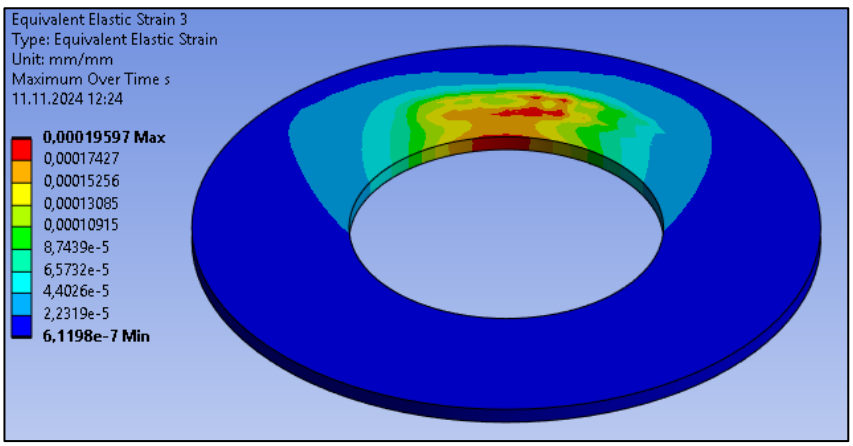

Figure 4.42. Equivalent elastic strain for case-7

Analysis results of case-8;

Equivalent stress is 40.502 MPa according to the analysis result.

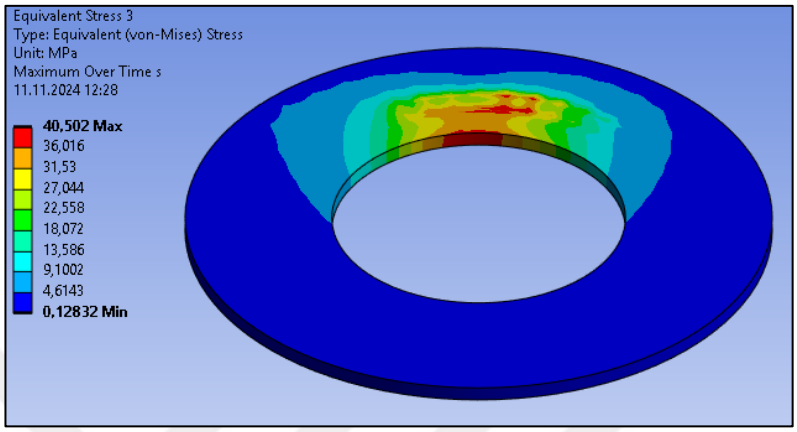

Figure 4.43. Equivalent stress for case-8

Total deformation is 85.661 mm according to the analysis result.

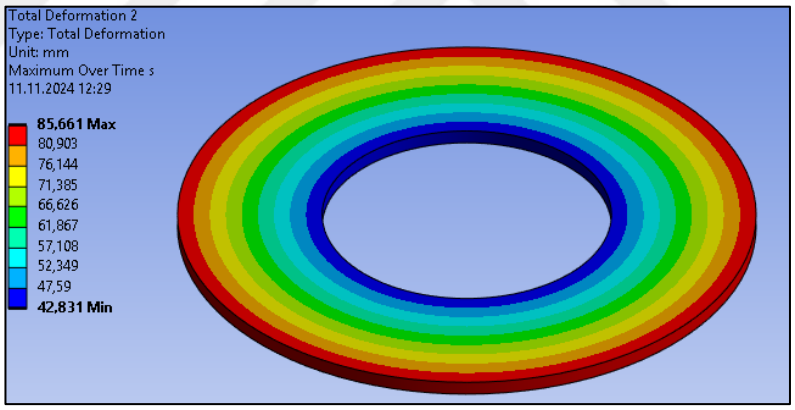

Figure 4.44. Total deformation for case-8

Directional deformation of X axis is 85.648 mm according to the analysis result.

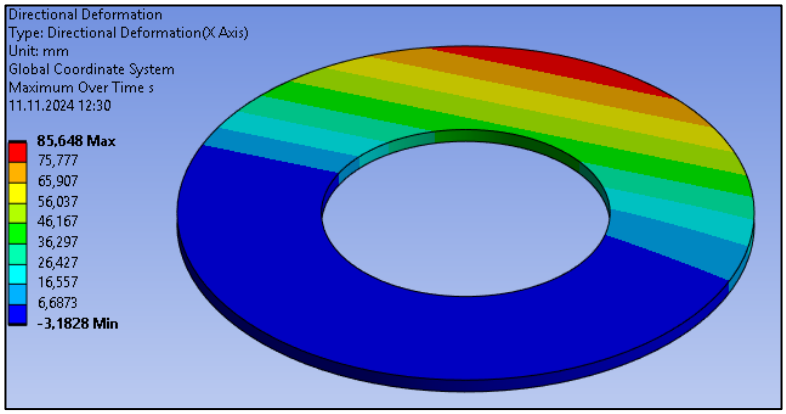

Figure 4.45. Directional deformation of X axis for case-8

Directional deformation of Z axis is 85.651 mm according to the analysis result.

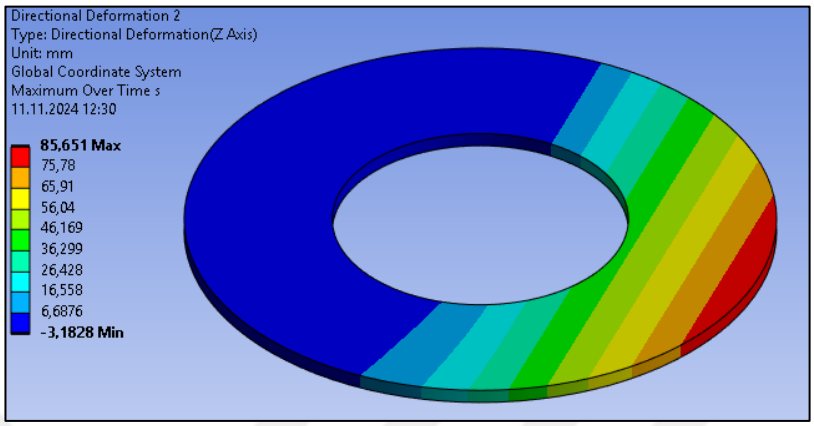

Figure 4.46. Directional deformation of Z axis for case-8

Directional deformation of Y axis is 0.0015008 mm according to the analysis result.

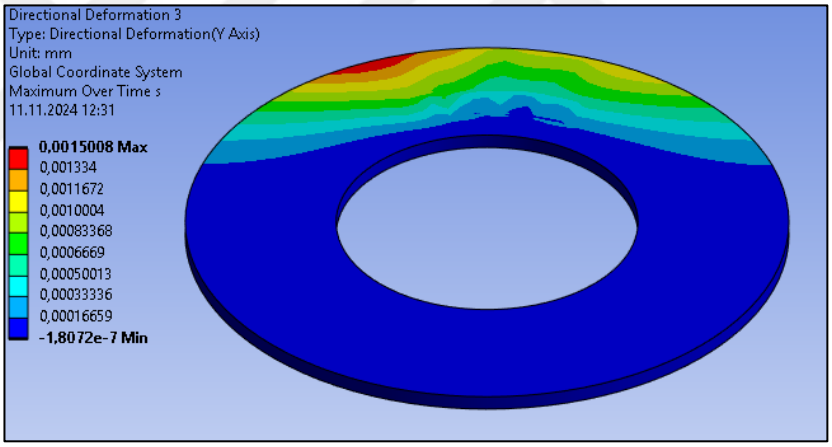

Figure 4.47. Directional deformation of Y axis for case-8

Equivalent elastic strain is 0.00021598 according to the analysis result.

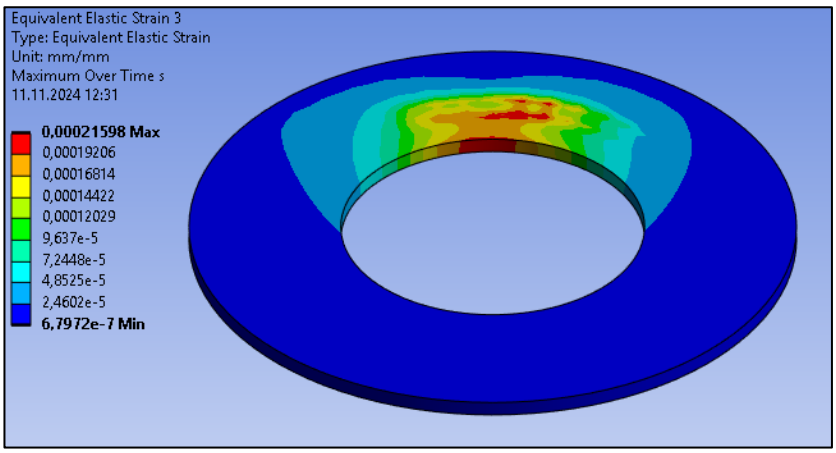

Figure 4.48. Equivalent elastic strain for case-8

Analysis results of case-9;

Equivalent stress is 39.365 MPa according to the analysis result.

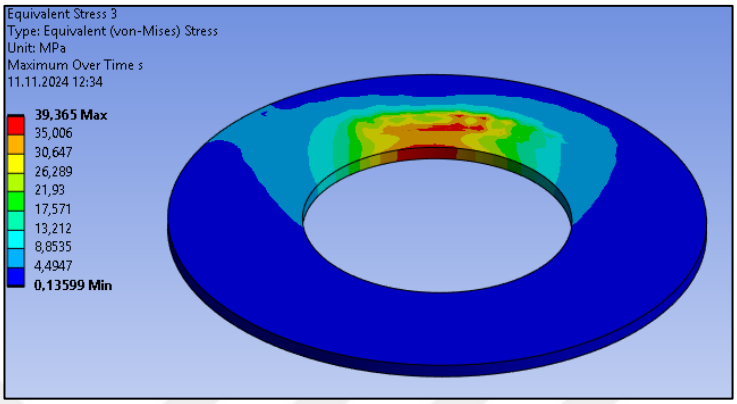

Figure 4.49. Equivalent stress for case-9

Total deformation is 85.661 mm according to the analysis result.

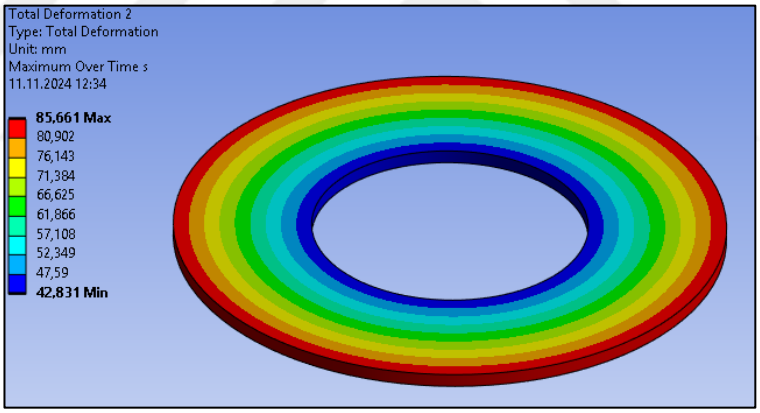

Figure 4.50. Total deformation for case-9

Directional deformation of X axis is 85.64 mm according to the analysis result.

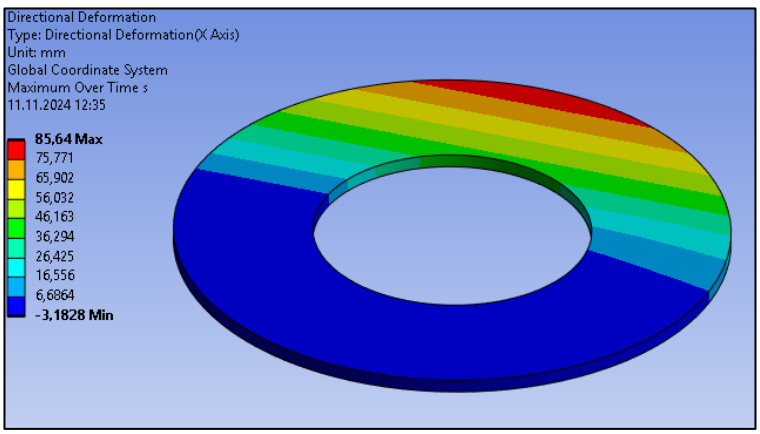

Figure 4.51. Directional deformation of X axis for case-9

Directional deformation of Z axis is 85.649 mm according to the analysis result.

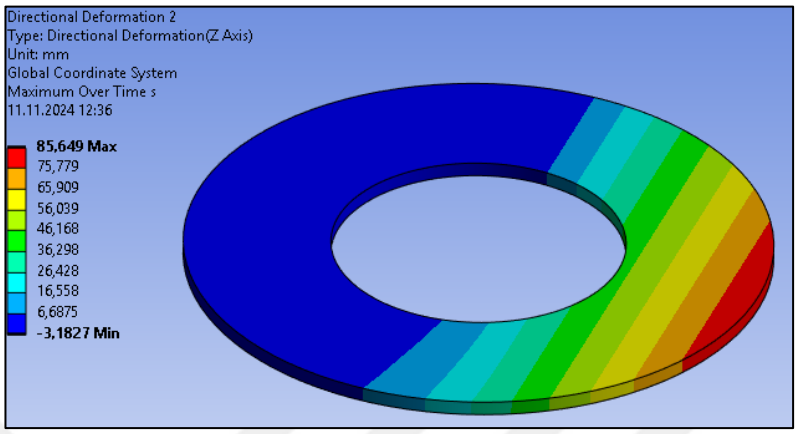

Figure 4.52. Directional deformation of Z axis for case-9

Directional deformation of Y axis is 0.0027236 mm according to the analysis result.

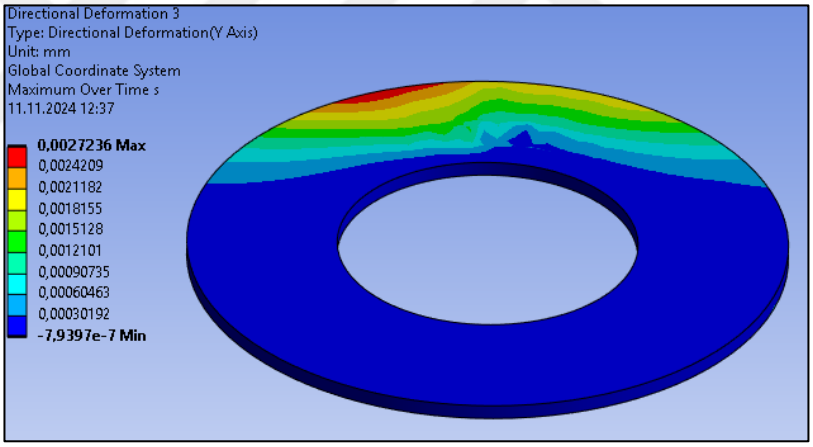

Figure 4.53. Directional deformation of Y axis for case-9

Equivalent elastic strain is 0.00056937 according to the analysis result.

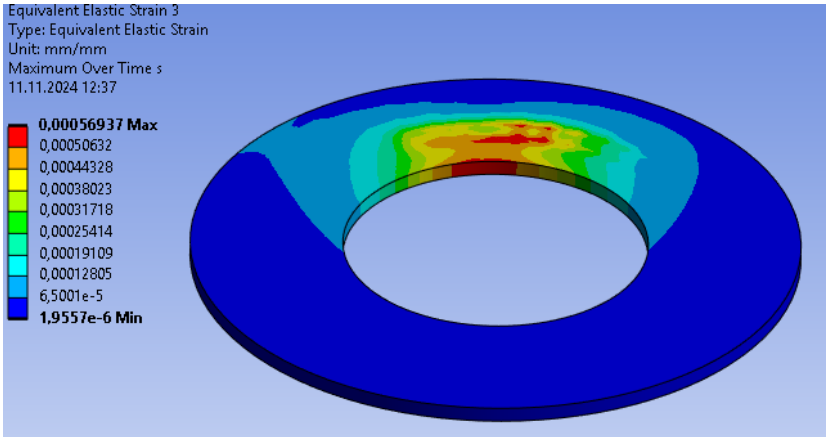

Figure 4.54. Equivalent elastic strain for case-9

Analysis results of case-10;

Equivalent stress is 37.613 MPa according to the analysis result.

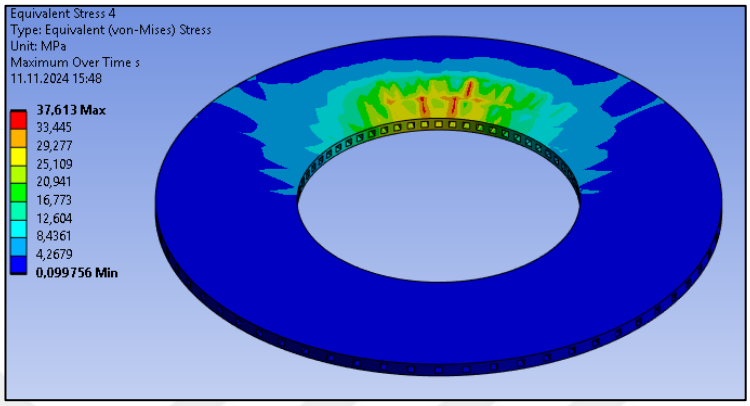

Figure 4.55. Equivalent stress for case-10

Total deformation is 85.662 mm according to the analysis result.

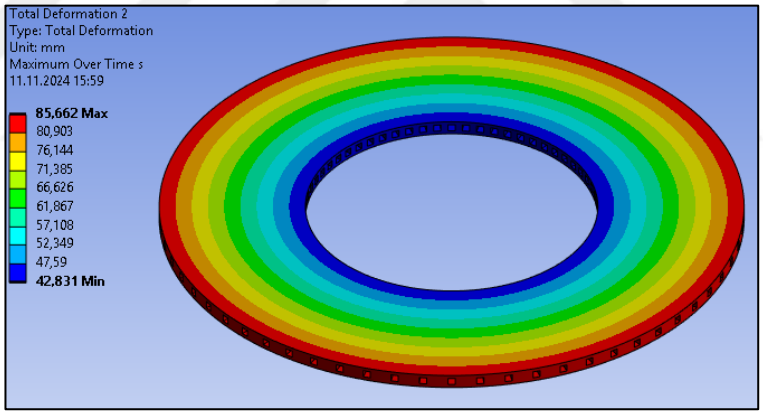

Figure 4.56. Total deformation for case-10

Directional deformation of X axis is 85.659 mm according to the analysis result.

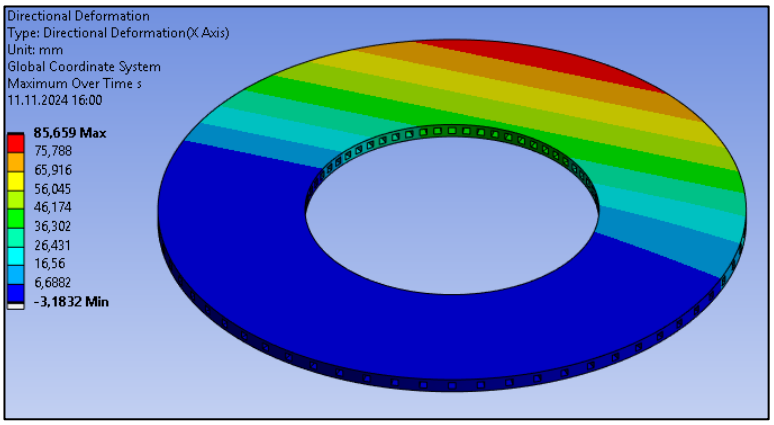

Figure 4.57. Directional deformation of X axis for case-10

Directional deformation of Z axis is 85.661 mm according to the analysis result.

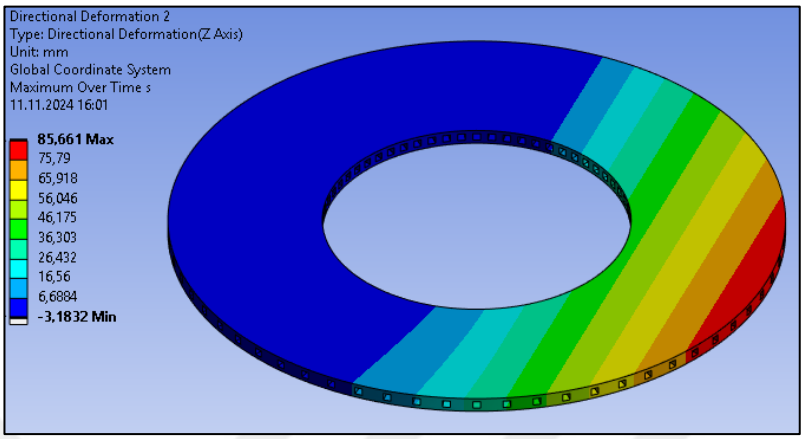

Figure 4.58. Directional deformation of Z axis for case-10

Directional deformation of Y axis is 0.0027779 mm according to the analysis result.

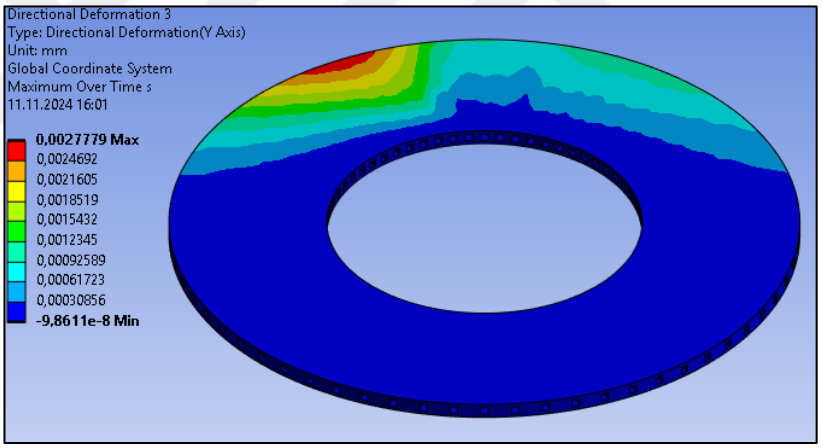

Figure 4.59. Directional deformation of Y axis for case-10

Equivalent elastic strain is 0.00018782 according to the analysis result.

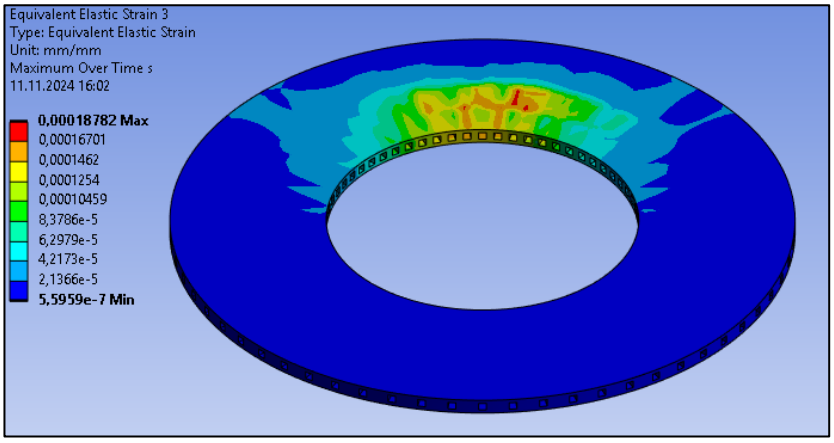

Figure 4.60. Equivalent elastic strain for case-10

Analysis results of case-11;

Equivalent stress is 36.881 MPa according to the analysis result.

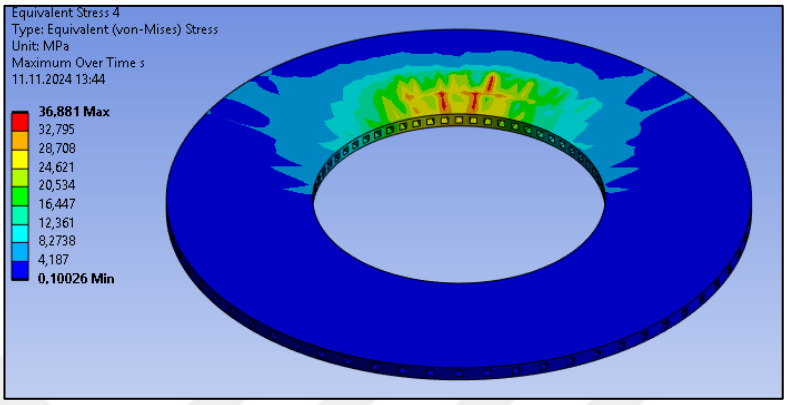

Figure 4.61. Equivalent stress for case-11

Total deformation is 85.662 mm according to the analysis result.

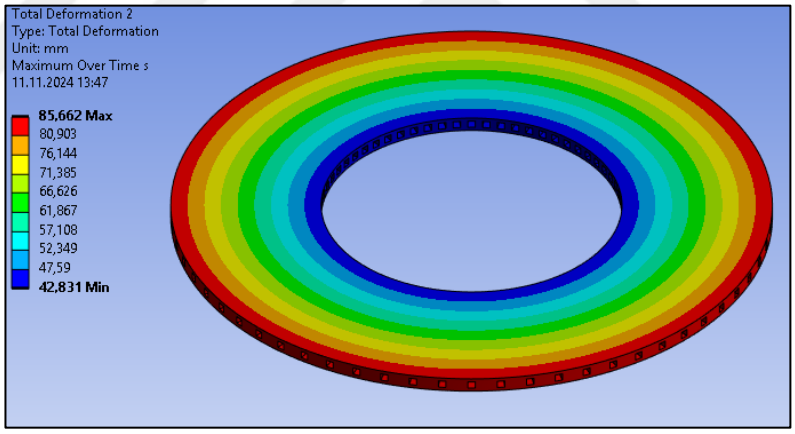

Figure 4.62. Total deformation for case-11

Directional deformation of X axis is 85.659 mm according to the analysis result.

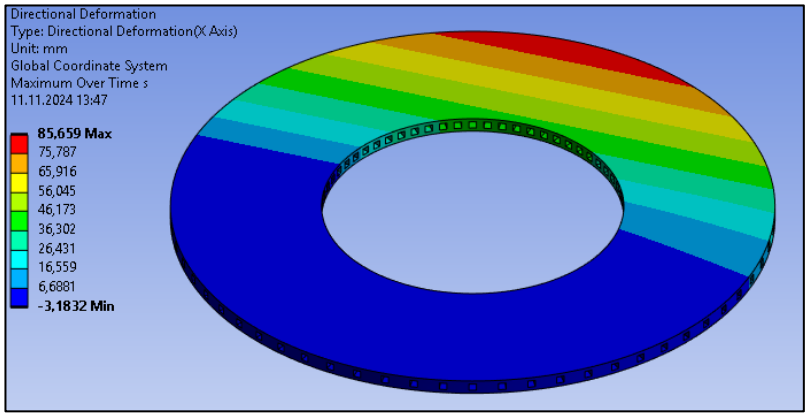

Figure 4.63. Directional deformation of X axis for case-11

Directional deformation of Z axis is 85.661 mm according to the analysis result.

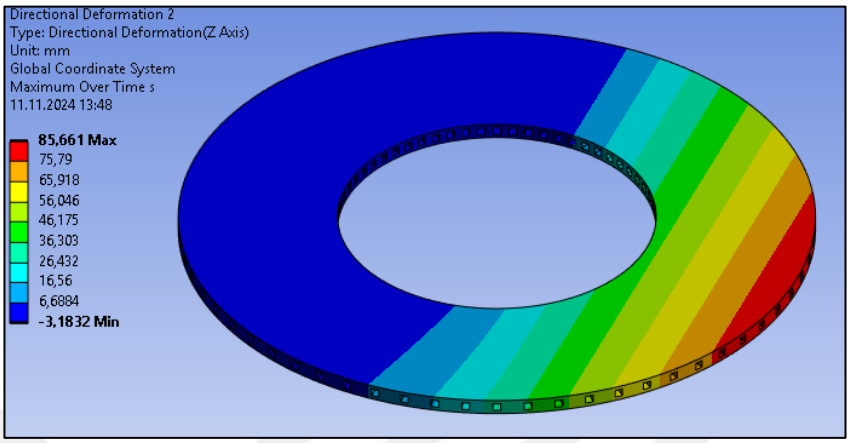

Figure 4.64. Directional deformation of Z axis for case-11

Directional deformation of Y axis is 0.0029053 mm according to the analysis result.

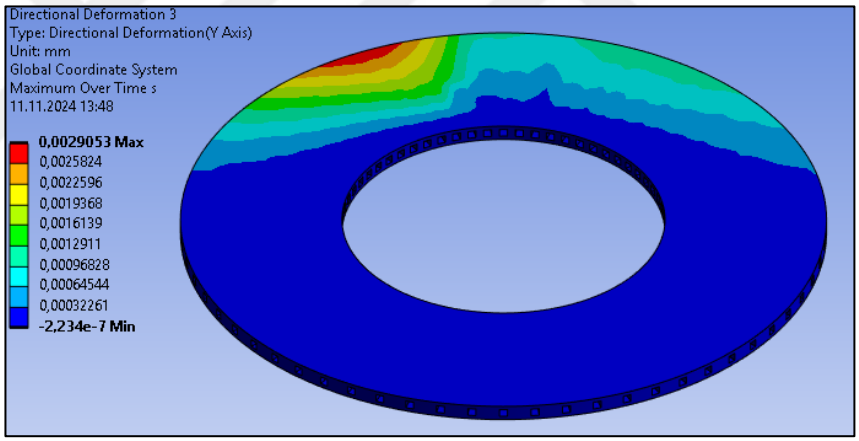

Figure 4.65. Directional deformation of Y axis for case-11

Equivalent elastic strain is 0.0002062 according to the analysis result.

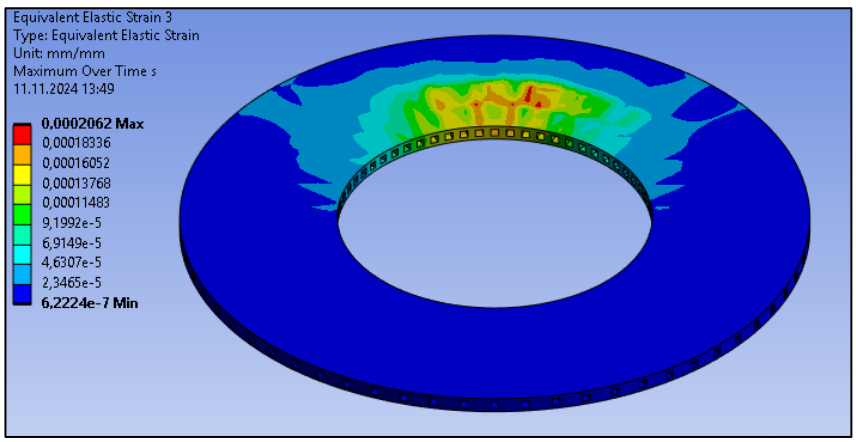

Figure 4.66. Equivalent elastic strain for case-11

Analysis results of case-12;

Equivalent stress is 34.939 MPa according to the analysis result.

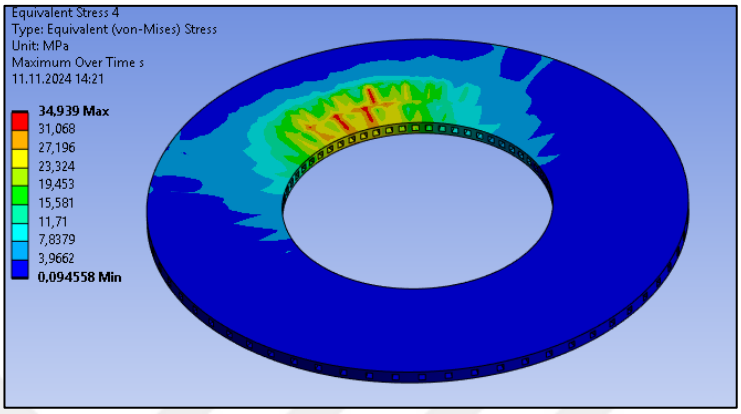

Figure 4.67. Equivalent stress for case-12

Total deformation is 85.661 mm according to the analysis result.

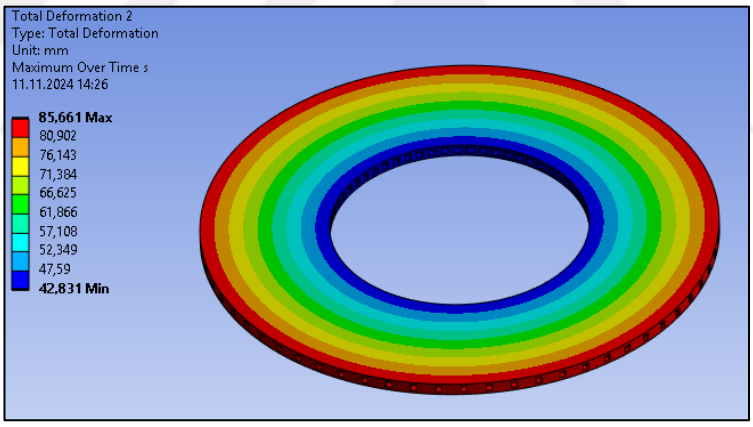

Figure 4.68. Total deformation for case-12

Directional deformation of X axis is 85.653 mm according to the analysis result.

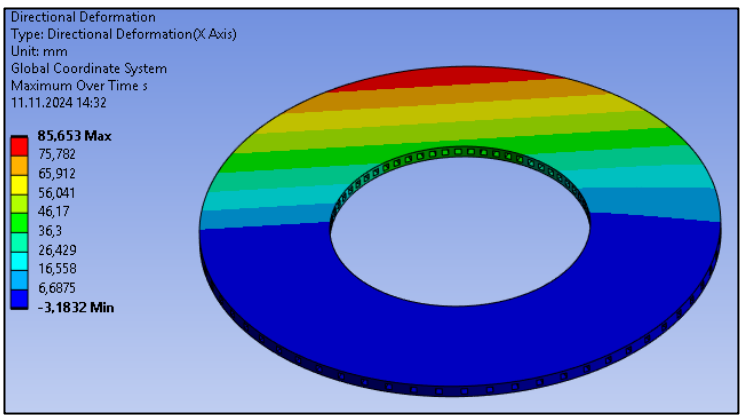

Figure 4.69. Directional deformation of X axis for case-12

Directional deformation of Z axis is 85.66 mm according to the analysis result.

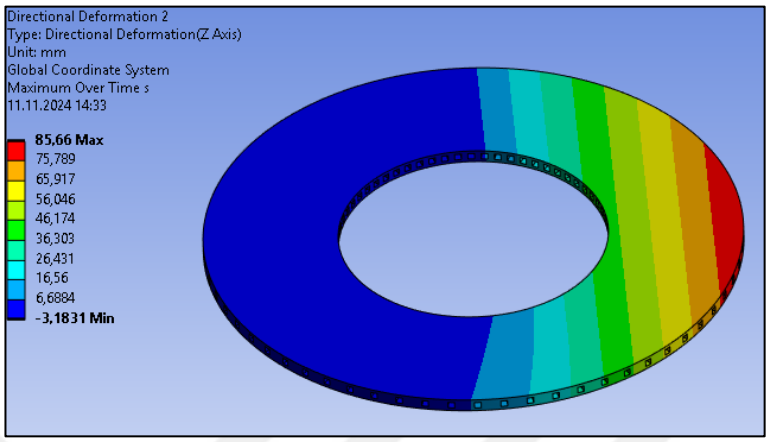

Figure 4.70. Directional deformation of Z axis for case-12

Directional deformation of Y axis is 0.0055514 mm according to the analysis result.

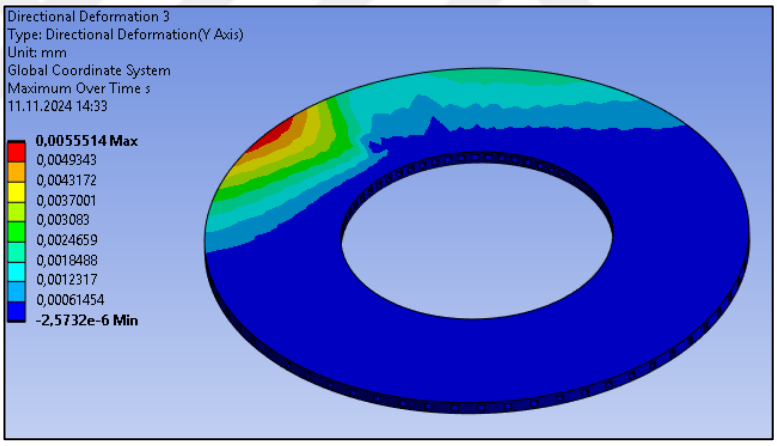

Figure 4.71. Directional deformation of Y axis for case-12

Equivalent elastic strain is 0.00052502 according to the analysis result.

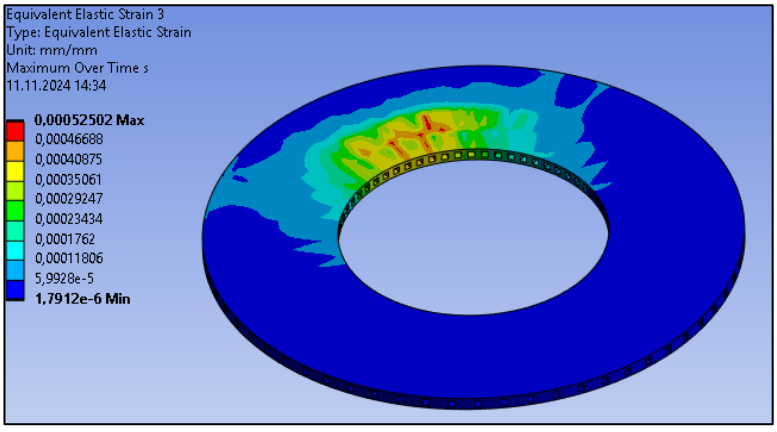

Figure 4.72. Equivalent elastic strain for case-12

Analysis results of case-13;

Equivalent stress is 164.27 MPa according to the analysis result.

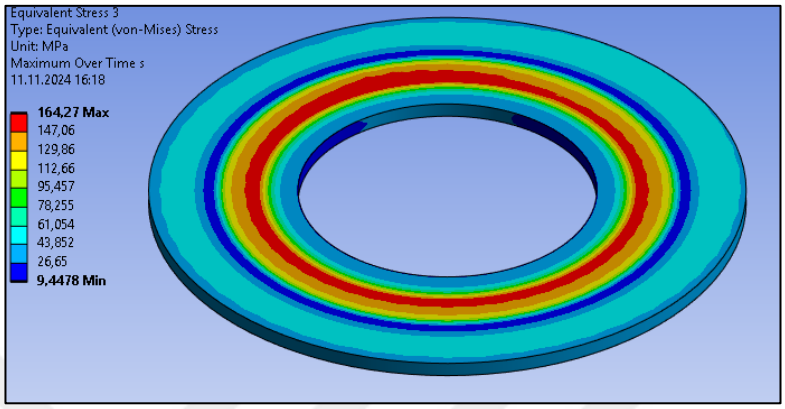

Figure 4.73. Equivalent stress for case-13

Total deformation is 85.67 mm according to the analysis result.

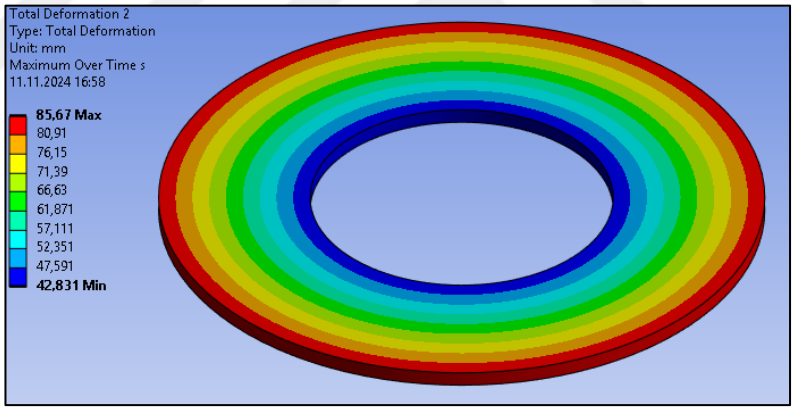

Figure 4.74. Total deformation for case-13

Directional deformation of X axis is 85.658 mm according to the analysis result.

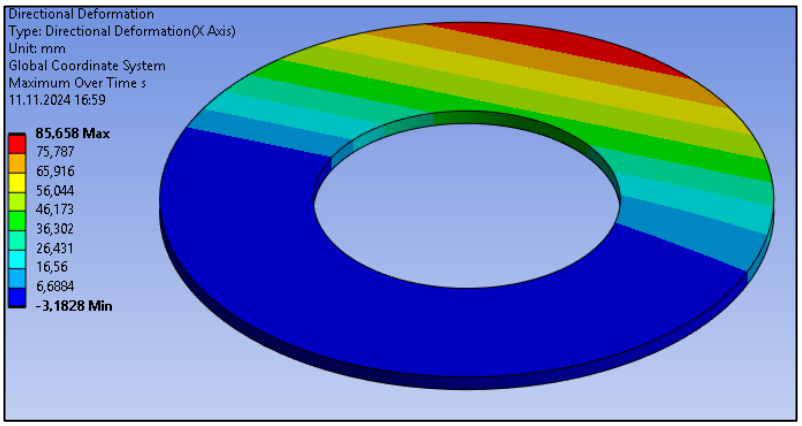

Figure 4.75. Directional deformation of X axis for case-13

Directional deformation of Z axis is 85.659 mm according to the analysis result.

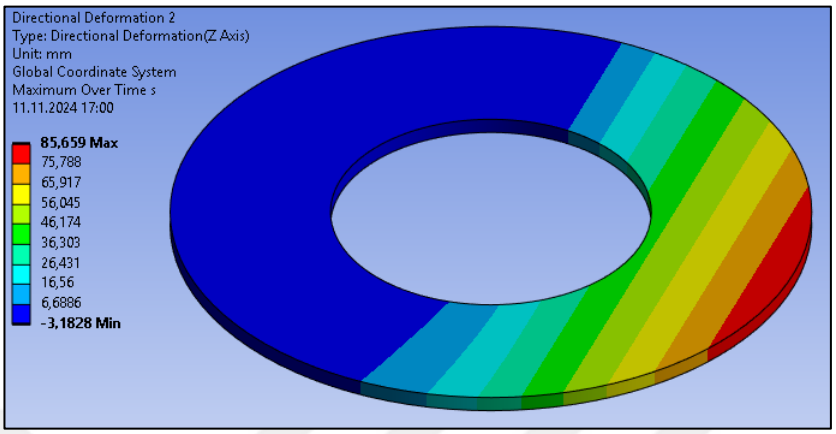

Figure 4.76. Directional deformation of Z axis for case-13

Directional deformation of Y axis is 0.0028298 mm according to the analysis result.

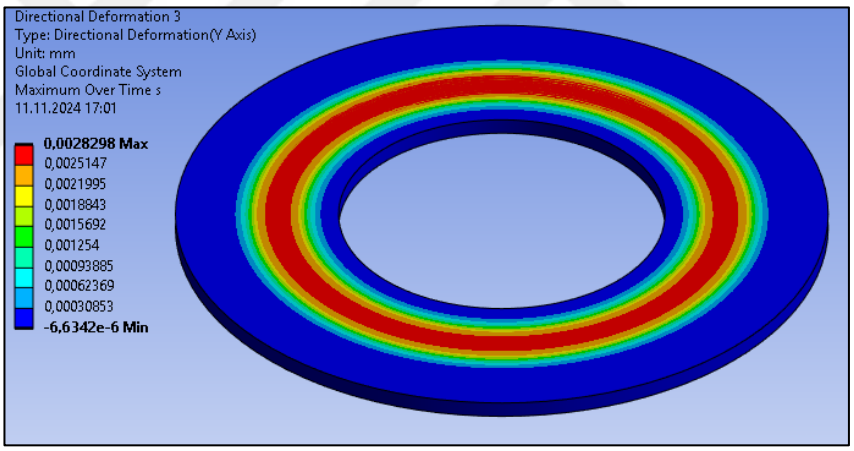

Figure 4.77. Directional deformation of Y axis for case-13

Equivalent elastic strain is 0.00078256 according to the analysis result.

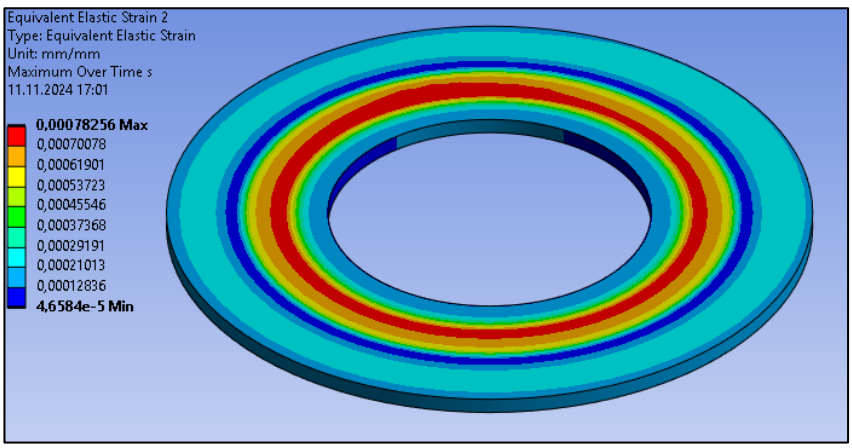

Figure 4.78. Equivalent elastic strain for case-13

Analysis results of case-14;

Equivalent stress is 218.95 MPa according to the analysis result.

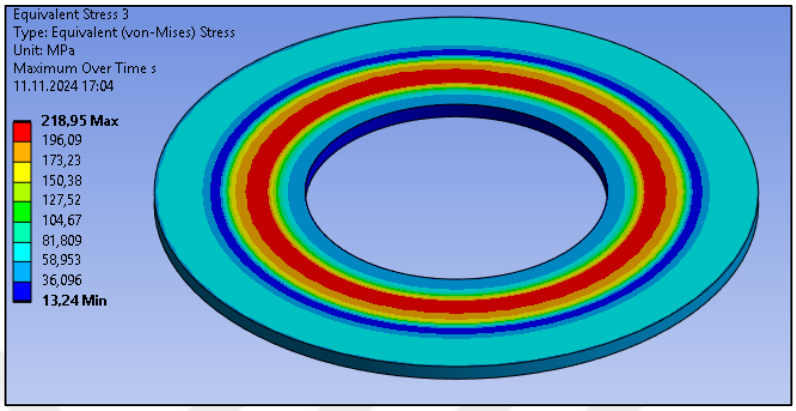

Figure 4.79. Equivalent stress for case-14

Total deformation is 85.675 mm according to the analysis result.

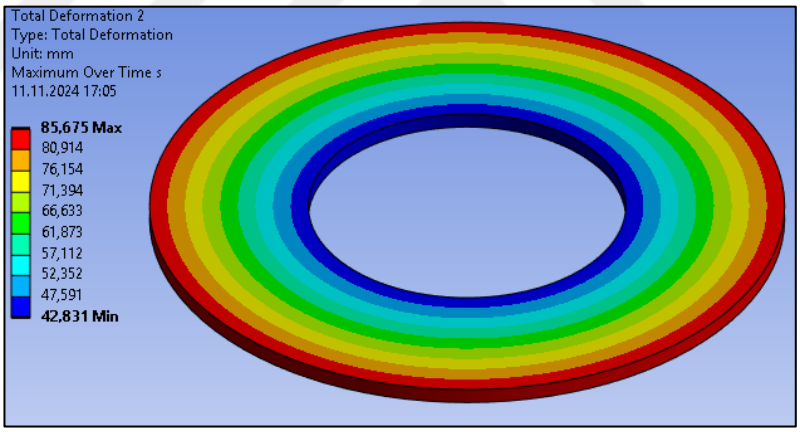

Figure 4.80. Total deformation for case-14

Directional deformation of X axis is 85.663 mm according to the analysis result.

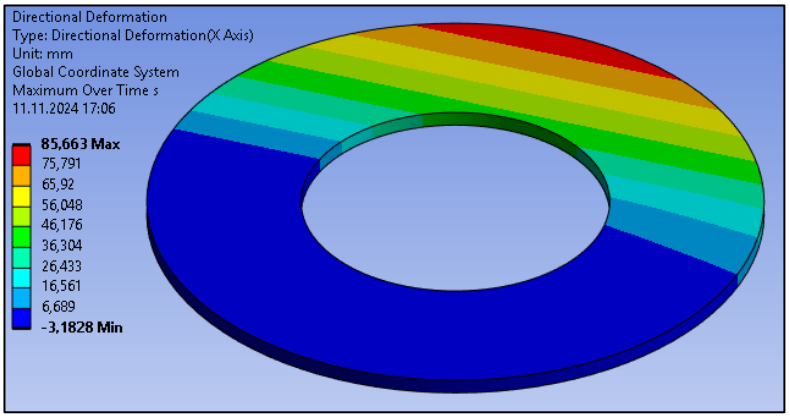

Figure 4.81. Directional deformation of X axis for case-14

Directional deformation of Z axis is 85.664 mm according to the analysis result.

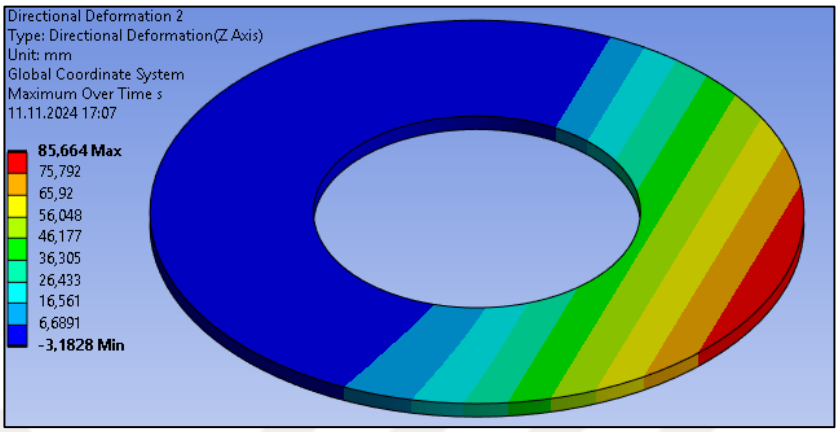

Figure 4.82. Directional deformation of Z axis for case-14

Directional deformation of Y axis is 0.0041476 mm according to the analysis result.

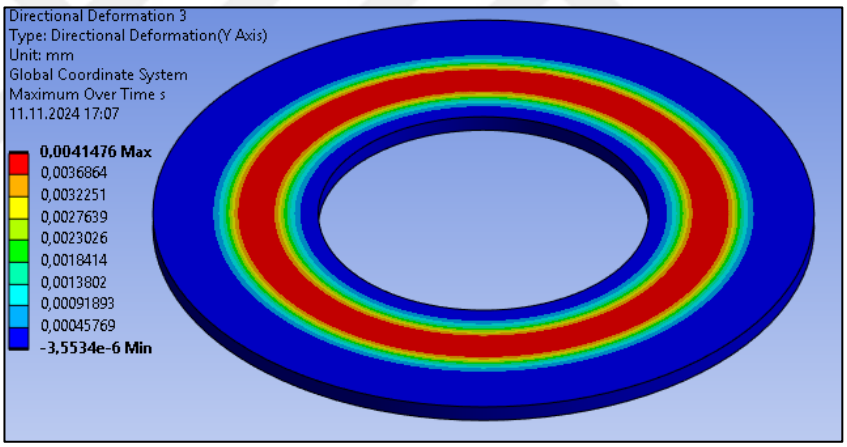

Figure 4.83. Directional deformation of Z axis for case-14

Equivalent elastic strain is 0.00011524 according to the analysis result.

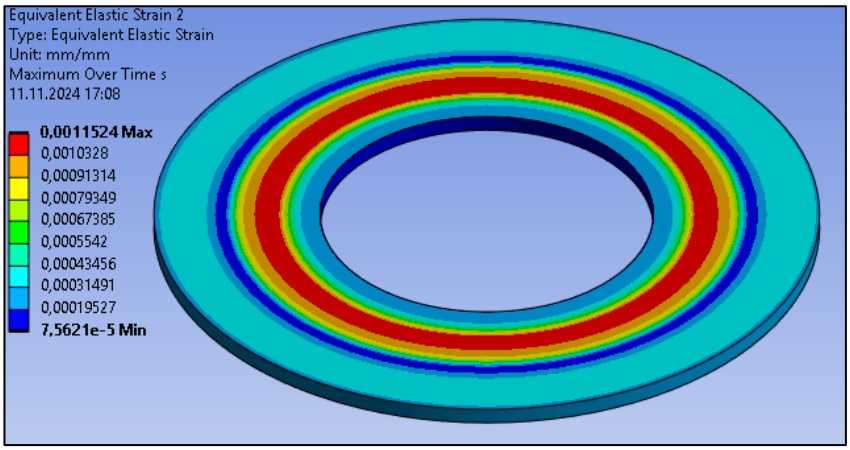

Figure 4.84. Equivalent elastic strain for case-14

Analysis results of case-15;

Equivalent stress is 93.857 MPa according to the analysis result.

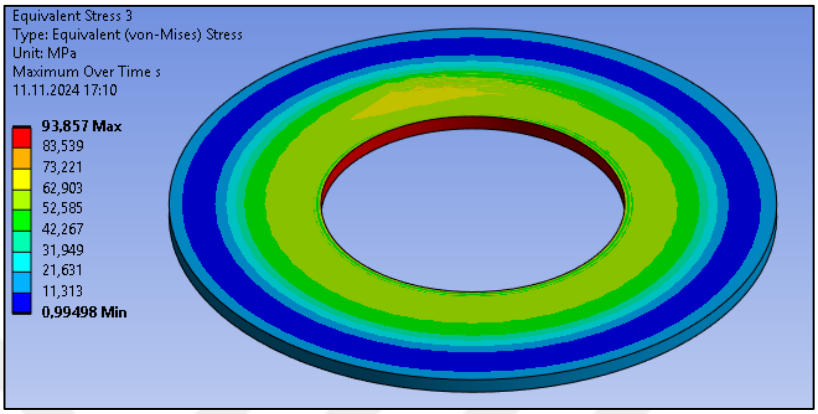

Figure 4.85. Equivalent stress for case-15

Total deformation is 85.683 mm according to the analysis result.

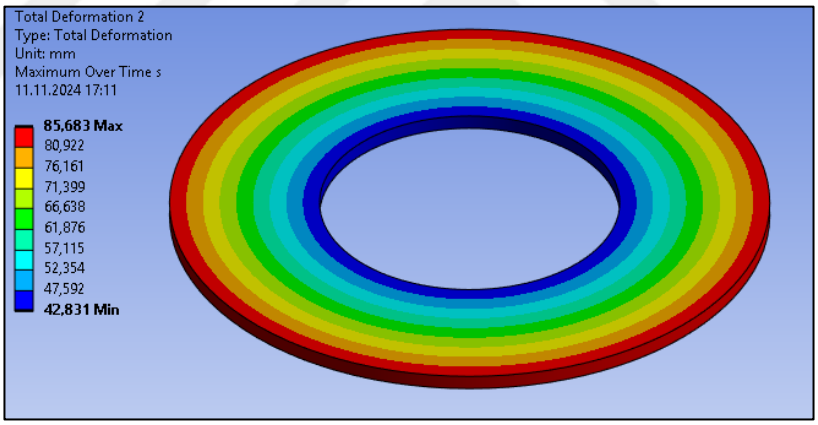

Figure 4.86. Total deformation for case-15

Directional deformation of X axis is 85.667 mm according to the analysis result.

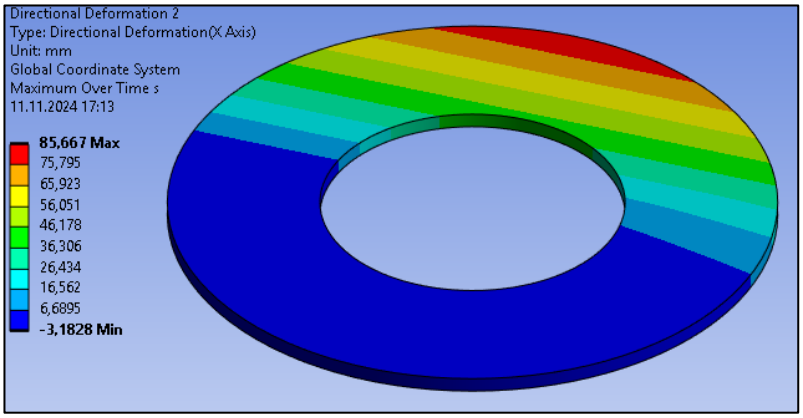

Figure 4.87. Directional deformation of X axis for case-15

Directional deformation of Z axis is 85.672 mm according to the analysis result

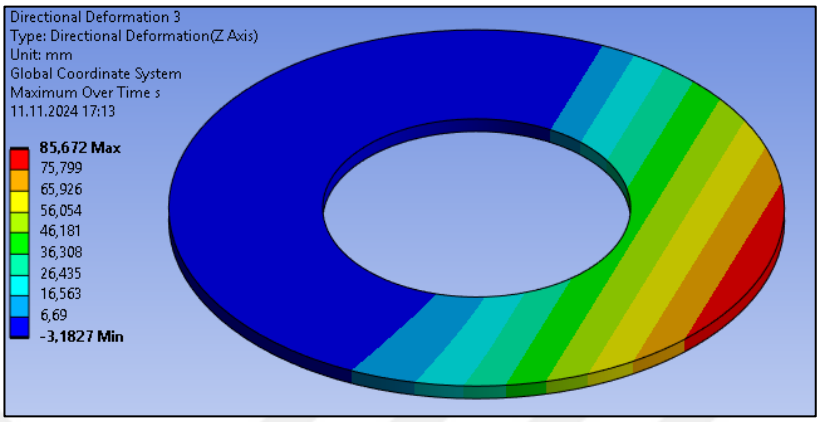

Figure 4.88. Directional deformation of Z axis for case-15

Directional deformation of Y axis is 0.0040975 mm according to the analysis result.

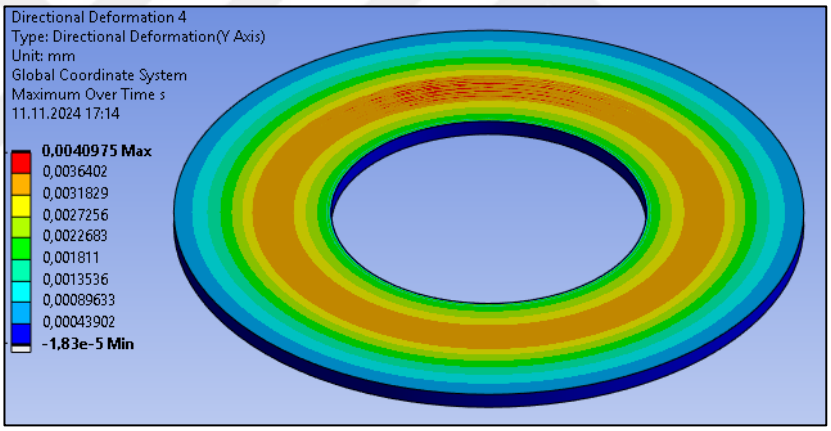

Figure 4.89. Directional deformation of Y axis for case-15

Equivalent elastic strain is 0.001341 according to the analysis result.

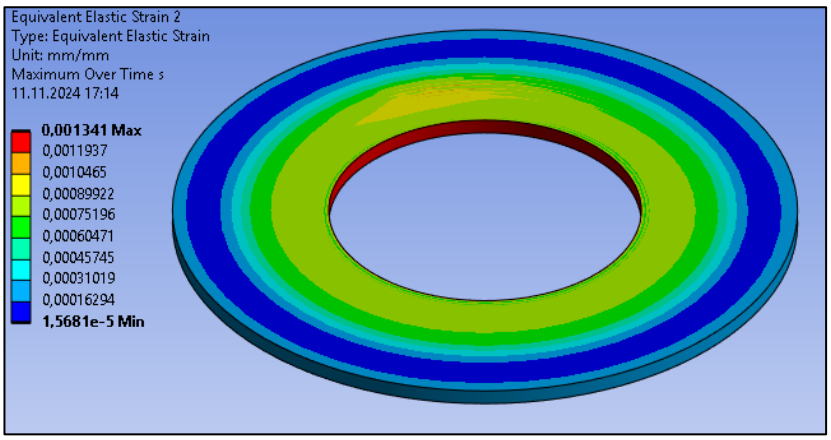

Figure 4.90. Equivalent elastic strain for case-15

Analysis results of case-16;

Equivalent stress is 212.03 MPa according to the analysis result.

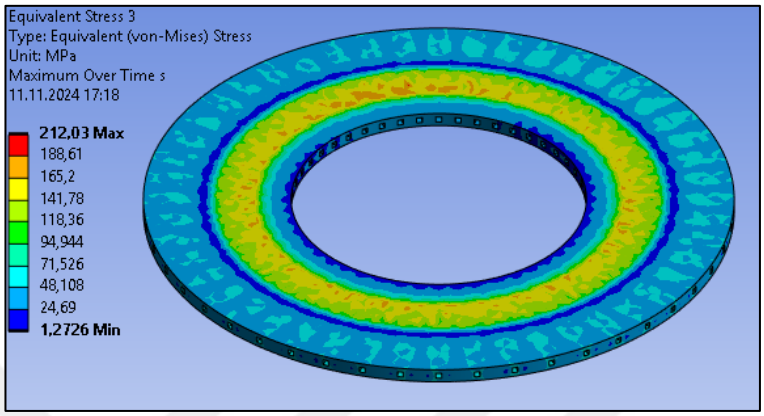

Figure 4.91. Equivalent stress for case-16

Total deformation is 85.671 mm according to the analysis result.

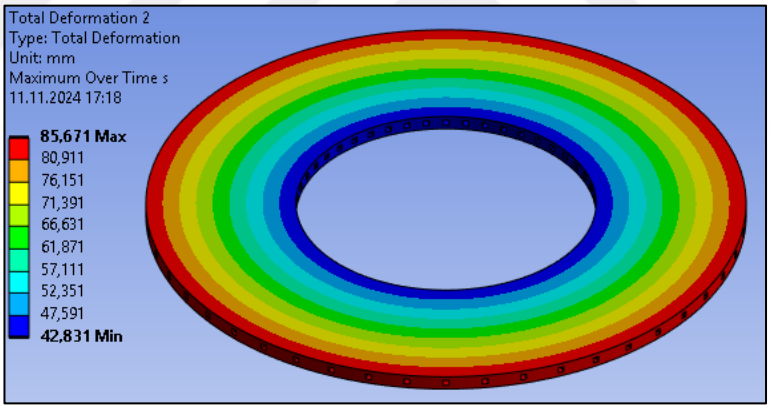

Figure 4.92. Total deformation for case-16

Directional deformation of X axis is 85.669 mm according to the analysis result.

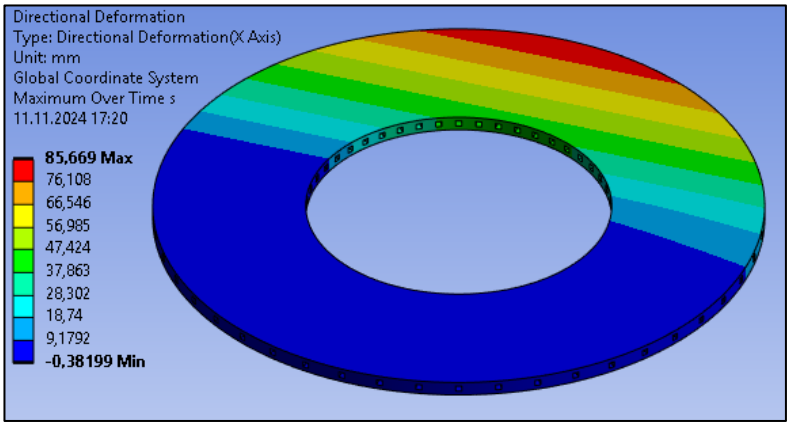

Figure 4.93. Directional deformation of X axis for case-16

Directional deformation of Z axis is 85.67 mm according to the analysis result.

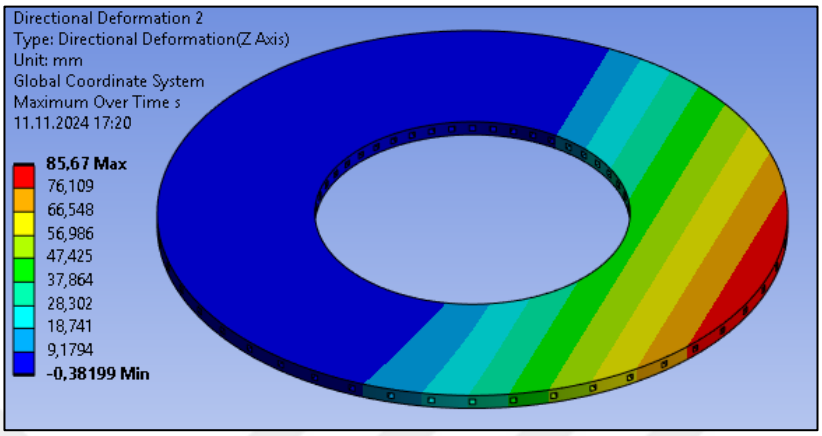

Figure 4.94. Directional deformation of Z axis for case-16

Directional deformation of Y axis is 0.0030871 mm according to the analysis result.

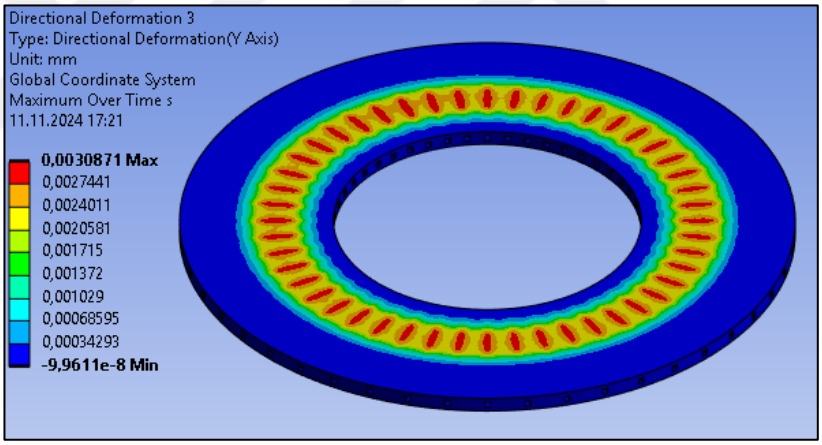

Figure 4.95. Directional deformation of Y axis for case-16

Equivalent elastic strain is 0.0010626 according to the analysis result.

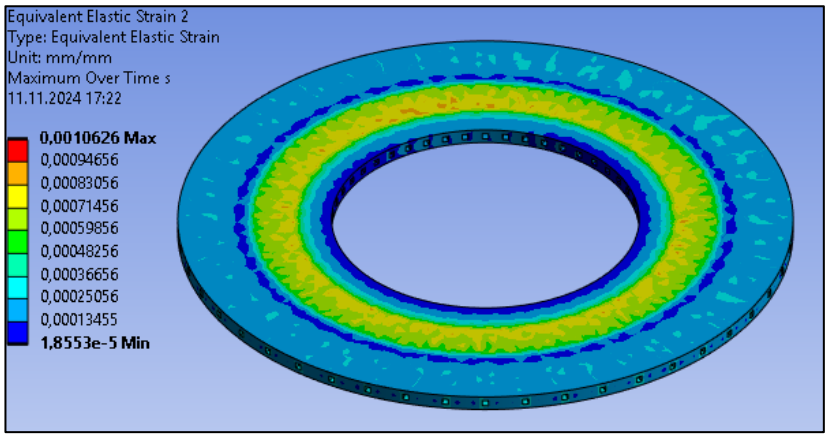

Figure 4.96. Equivalent elastic strain for case-16

Analysis results of case-17;

Equivalent stress is 289.42 MPa according to the analysis result.

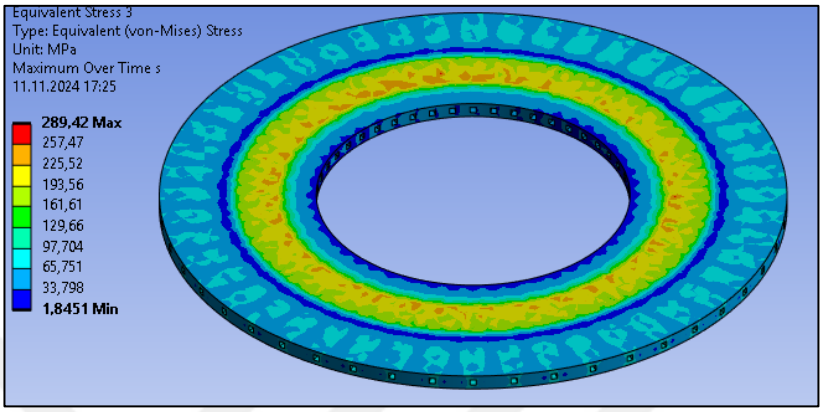

Figure 4.97. Equivalent stress for case-17

Total deformation is 85.676 mm according to the analysis result.

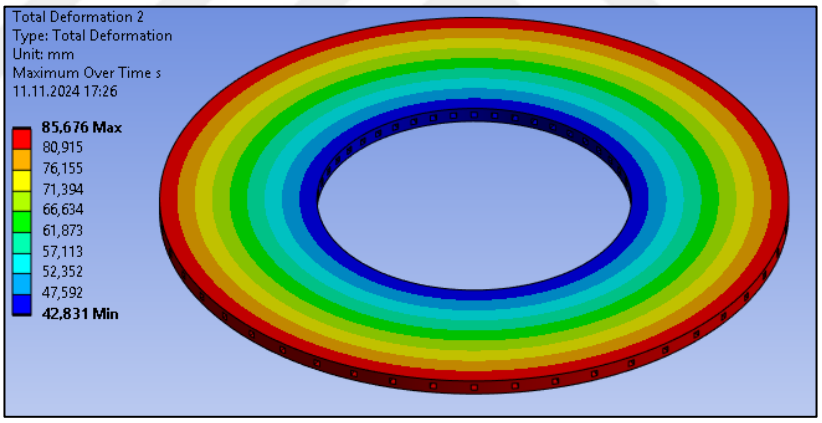

Figure 4.98. Total deformation for case-17

Directional deformation of X axis is 85.673 mm according to the analysis result.

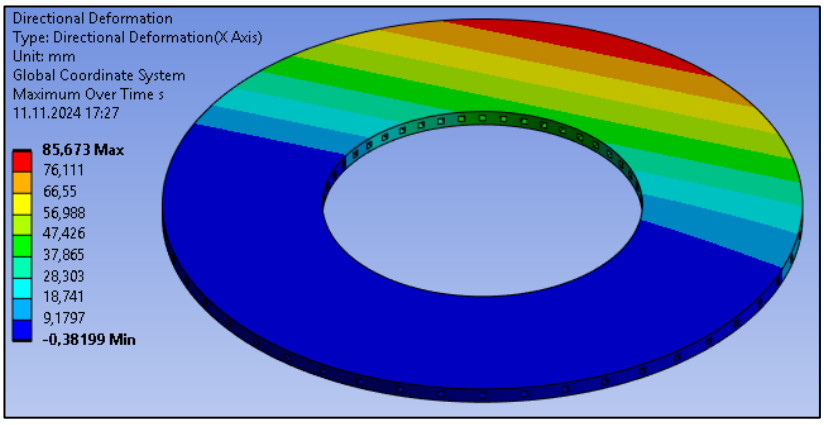

Figure 4.99. Directional deformation of X axis for case-17

Directional deformation of Z axis is 85.675 mm according to the analysis result.

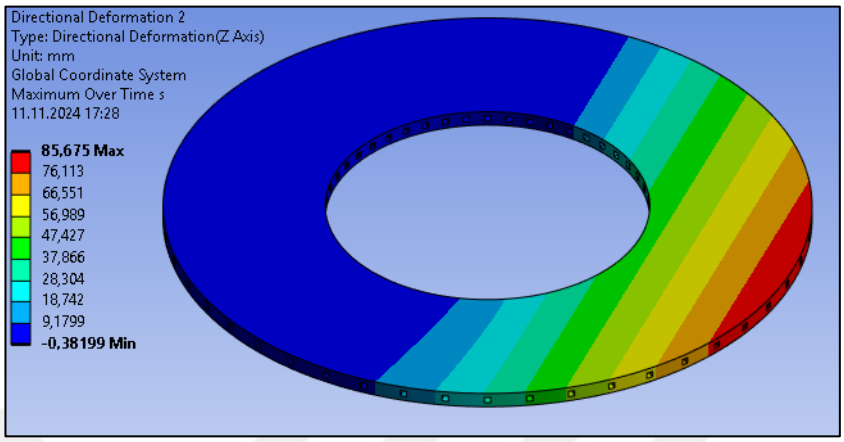

Figure 4.100. Directional deformation of Z axis for case-17

Directional deformation of Y axis is 0.0047577 mm according to the analysis result.

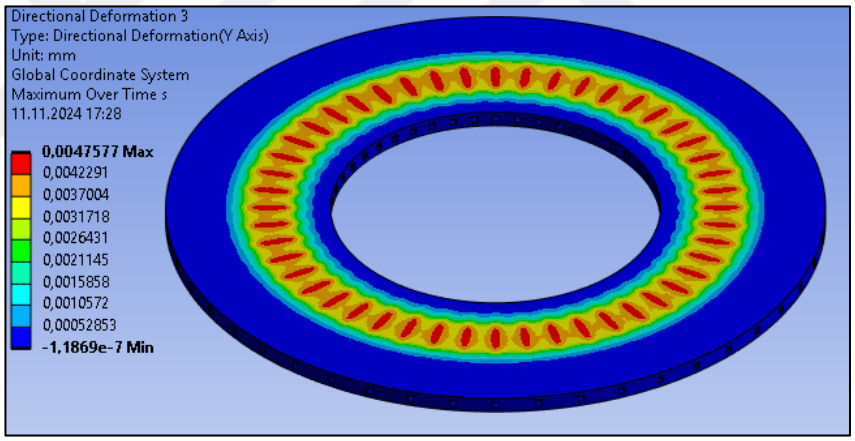

Figure 4.101. Directional deformation of Y axis for case-17

Equivalent elastic strain is 0.0016016 according to the analysis result.

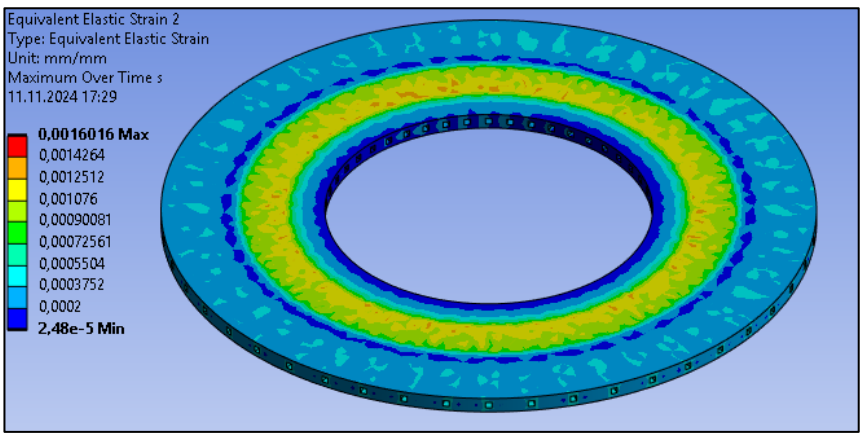

Figure 4.102. Equivalent elastic strain for case-17

Analysis results of case-18;

Equivalent stress is 151.3 MPa according to the analysis result.

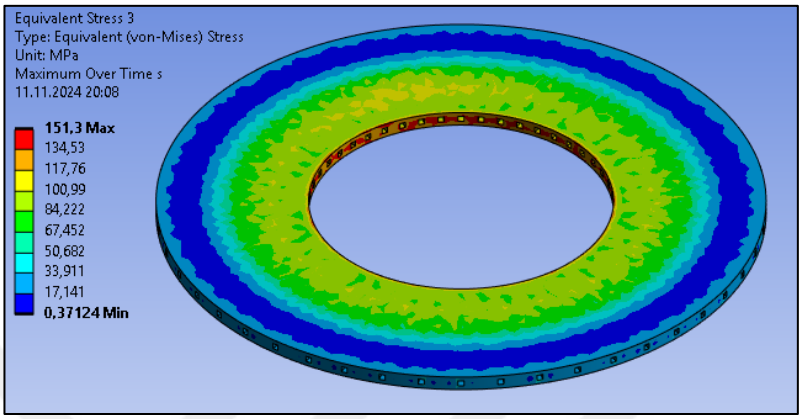

Figure 4.103. Equivalent stress for case-18

Total deformation is 85.698 mm according to the analysis result.

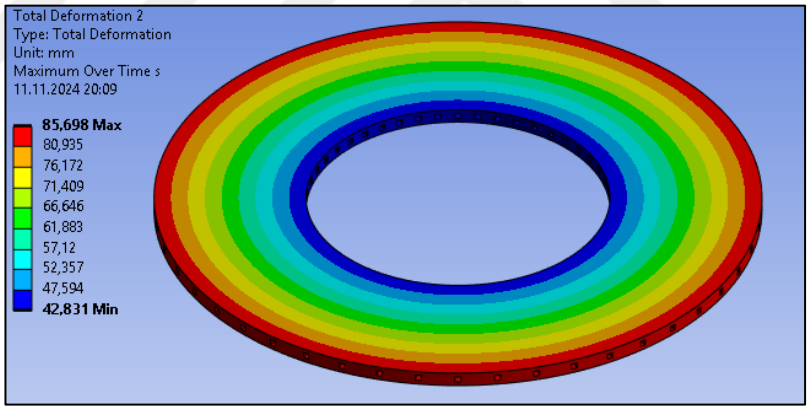

Figure 4.104. Total deformation for case-18

Directional deformation of X axis is 85.691 mm according to the analysis result.

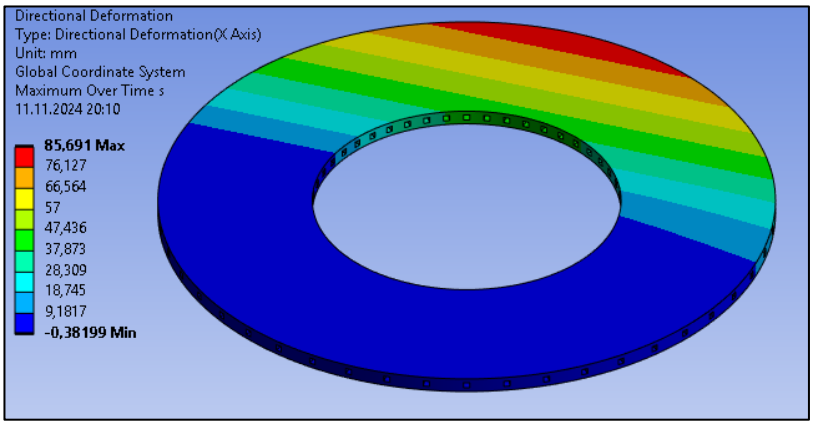

Figure 4.105. Directional deformation of X axis for case-18

Directional deformation of Z axis is 85.697 mm according to the analysis result.

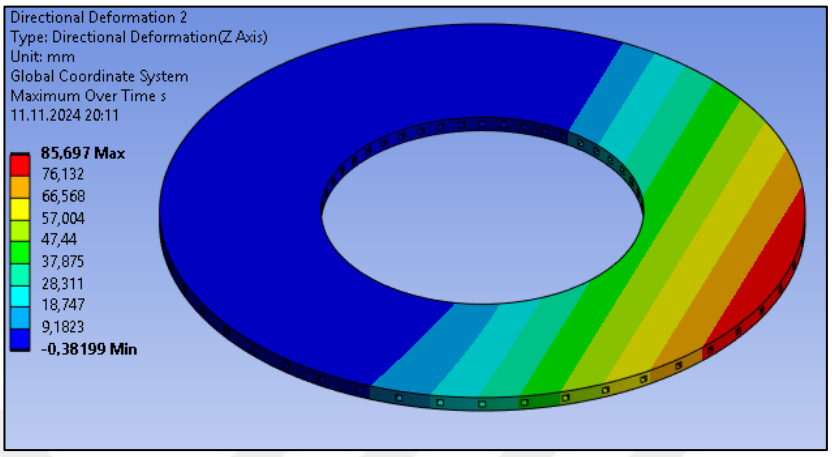

Figure 4.106. Directional deformation of Z axis for case-18

Directional deformation of Y axis is 0.0063273 mm according to the analysis result.

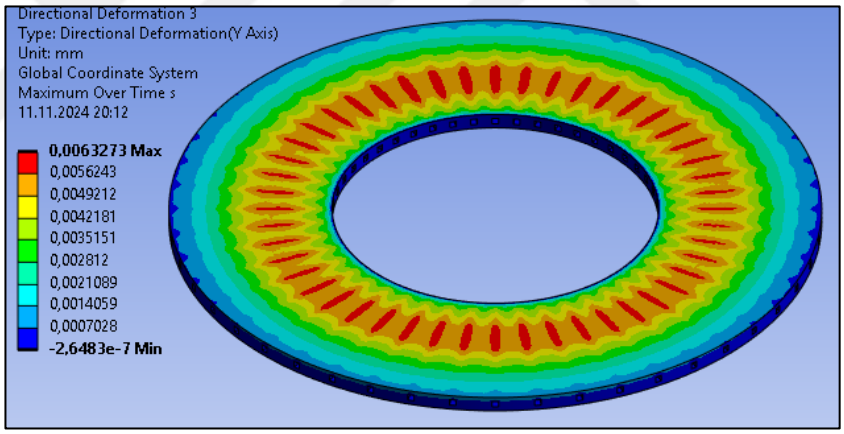

Figure 4.107. Directional deformation of Y axis for case-18

Equivalent elastic strain is 0.0021641 according to the analysis result.

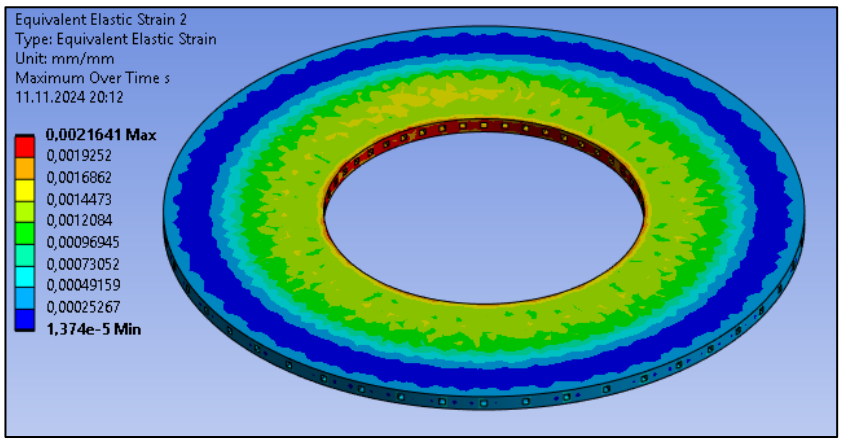

Figure 4.108. Equivalent elastic strain for case-18

The results of the analysis run from case-1 to case-12 according to the structural analysis method are given in the table below.

Table 4.1. Analysis results of structural analysis

Braking Pressure	Geometry	Material Quality	Cases	Equivalent Stress (MPa)	Directional Deformation of Y Axis (mm)	Equivalent Elastic Strain
10 MPa	Solid	Structural S.	Case-1	24.263	0.0070521	0.00011588
		Stainless S.	Case-2	24.022	0.0076362	0.00012681
		Aluminum A.	Case-3	21.641	0.015291	0.00031096
	Ventilated	Structural S.	Case-4	37.613	0.0027779	0.00018782
		Stainless S.	Case-5	36.881	0.0029053	0.0002062
		Aluminum A.	Case-6	34.939	0.0055514	0.00052502
20 MPa	Solid	Structural S.	Case-7	40.615	0.0013977	0.00019597
		Stainless S.	Case-8	40.502	0.0015008	0.00021598
		Aluminum A.	Case-9	39.365	0.0027236	0.00056937
	Ventilated	Structural S.	Case-10	37.613	0.0027779	0.00018782
		Stainless S.	Case-11	36.881	0.0029053	0.0002062
		Aluminum A.	Case-12	34.939	0.0055514	0.00052502

As seen in table 4.1., there was an increase in equivalent stress values when a ventilated geometry was preferred over a solid geometry. It was also observed that the directional deformation in the direction of the brake pressure applied also increased. When material grades were compared, the equivalent stress value of aluminum alloy was lower than that of structural steel and stainless steel. The reason for this was that aluminum material shows more flexible behavior under pressures or forces. We can also understand the accuracy of this by

looking at equivalent strain values. While the equivalent stress value of the aluminum alloy brake disc was lower than that of brake discs of other material qualities, the equivalent strain and directional deformation values are correspondingly higher.

In addition to all these, the brake pressure value was doubled, and the analysis results were examined. Equivalent stress, equivalent strain and directional deformation values were also increased for all material qualities and geometries.

The results of the analysis ran from case-13 to case-18 according to the thermal and structural analysis method were given in the table below.

Table 4.2. Analysis results of thermal and structural analysis

Braking Pressure	**Geometry**	**Material Quality**	**Cases**	**Equivalent Stress (MPa)**	**Directional Deformation of Y Axis (mm)**	**Equivalent Elastic Strain**
10 MPa	Solid	Structural S.	Case-13	164.27	0.0028298	0.00078256
		Stainless S.	Case-14	218.95	0.0041476	0.00011524
		Aluminum A.	Case-15	93.857	0.0040975	0.001341
	Ventilated	Structural S.	Case-16	212.03	0.0030871	0.0010626
		Stainless S.	Case-17	289.42	0.0047577	0.0016016
		Aluminum A.	Case-18	151.3	0.0063273	0.0021641

When thermal effects were included in the analysis, the effect of the thermal conductivity coefficients given in table 3.4. was reflected in the analysis results. An increase in the equivalent stress value of the stainless steel material was observed under thermal effects. But again, due to the flexibility of aluminum alloy material, the equivalent stress value in this material was low compared to other materials. This can again be verified by looking at the increase in equivalent strain values.

This study aimed to enhance the efficiency of disc brakes by optimizing their design through computational methods. The main objectives were to improve the geometry of the disc and choose the best material to achieve an optimal design.

Design Process and Tools

- **Design Creation:** Initial disc designs were developed using computer-aided design (CAD) software.
- **Simulation Tools:** The Finite Element Method (FEM) was used to simulate and evaluate these designs.
- **Material Selection:** Different materials were tested, including aluminum alloy steel, stainless steel, and structural steel.

Key Parameters and Metrics

- **Thermal Conductivity:** A critical factor for disc brake efficiency.
- **Geometry Variations:** Various geometric configurations of the disc were tested to identify the most efficient design.

Comparative Analysis

- **Material Quality:**
    - **Aluminum Alloy Steel:** Balanced trade-off between weight and thermal conductivity.
    - **Stainless Steel:** High durability and thermal resistance.
    - **Structural Steel:** Good mechanical properties but less optimal thermal performance.
- **Geometry Impact:** Different disc geometries had a significant impact on thermal conductivity and overall performance.

Results Summary

- **Optimal Design:** The study identified an optimal combination of disc geometry and material that maximized thermal conductivity and efficiency.
- **Material Efficiency:** Aluminum alloy steel was found to be the most efficient material for disc brake design, offering the best balance between thermal performance and weight.
- **Performance Evaluation:** The optimized design showed substantial improvements in thermal conductivity, which is crucial for effective disc brake performance.

5. DISCUSSION

This study highlights how computational methods can significantly improve disc brake design. By using CAD, and FEM, we refined both the geometry and material selection of disc brakes, resulting in better thermal conductivity and overall efficiency. Aluminum alloy steel stood out as the most effective material, offering a good balance of weight, durability, and thermal performance.

One of the main takeaways is the crucial role that material properties play in the thermal management of disc brakes. Aluminum alloy steel, with its excellent thermal conductivity and mechanical strength, outperformed stainless steel and structural steel. This finding emphasizes the importance of choosing the right materials for components that need to handle high temperatures and mechanical stress.

Geometric optimization was another key focus. We found that even small changes in the design could lead to significant performance improvements. This underscores the value of detailed simulations and analysis, allowing for precise tweaks that can make a big difference.

Advanced cooling mechanisms and special coatings could further improve thermal management. Additionally, integrating machine learning and artificial intelligence into the design and simulation process could speed up development and lead to more sophisticated optimizations.

In conclusion, while this study has made great strides in optimizing disc brake design, it also opens the door to many future improvements. By continuing to innovate and explore new materials, designs, and technologies, we can further enhance automotive braking systems, making them safer and more efficient.

6. CONCLUSION AND RECOMMENDATIONS

In conclusion, this study managed to enhance disc brake design using computational methods, revealing that aluminum alloy steel, when paired with the right geometric configuration, greatly improves thermal conductivity and overall efficiency. These findings highlight how crucial material selection and design precision are in boosting brake performance. This work underscores the importance of advanced engineering tools and simulations in creating high-performance automotive components. By carefully examining different materials and designs, the research provides a solid foundation for future brake system innovations. The improved thermal conductivity from the optimized design not only boosts performance but also enhances the safety and durability of disc brakes. This study sets the stage for ongoing advancements in automotive engineering, showing how essential computational techniques are in developing more efficient and dependable braking systems.

For future research, it is suggested to explore the new materials and composites that could offer even better thermal and mechanical properties. Understanding how these optimized disc designs hold up over time in real-world conditions could give us a clearer picture of their practical use. Future research might also look into advanced cooling mechanisms or special coatings to improve how disc brakes manage heat. Additionally, using machine learning and artificial intelligence in the design and simulation process could speed up and enhance optimizations for the next generation of automotive braking systems.

REFERENCES

Manjunath T V, Dr. Suresh P M (2013). Structural and Thermal Analysis of Rotor Disc of Disc Brake. *International Journal of Innovative Research in Science, Engineering and Technology*, Vol.2. ISSN: 2319-8753.

Ameer Fareed Basha Shaik, Ch.Lakshmi Srinivas (2012). Structural and Thermal Analysis of Disc Brake With and Without Cross drilled Rotor of Race Car. *International Journal of Advanced Engineering Research and Studies*, Vol.1, PP 39-43.

S. Sarip (2013). Design Development of Lightweight Disc Brake for Regenerative Braking and Finite Element Analysis. *International Journal of Applied Physics and Mathematics*, Vol. 3, PP 52-58. https://doi.org/10.7763/ijapm.2013.v3.173

Guru Murthy Nathil, T N Charyulu (2012). Coupled Structural/ Thermal Analysis of Disc Brake. *IJRET*, Vol.2, PP 539-553. https://doi.org/10.15623/ijret.2012.0104004

V. Chengal Reddy, M. Gunasekhar Reddy (2013). Modeling and Analysis of FSAE Car Disc Brake Using FEM. *International Journal of Emerging Technology and Advanced Engineering*, Vol.3, PP 383-389.

Michal Kuciej, Piotr Grzes (2011). The Comparable Analysis of Temperature Distributions Assessment in Disc Brake Obtained Using Analytical Method and FE Model. *Journal of KONES Powertrain and Transport*, Vol.18, PP 236-250.

Antti Papinniemi, Joseph C.S. Lai (2007). Disc Brake Squeal, Progress and Challenges. *ICSV14, Australia*, PP 1-8.

F.Talati, S.Jalalifar (2008). Investigation of heat transfer phenomenon in a ventilated disc brake rotor with straight radial vanes. *journal of applied science* Vol.8 PP 3583-3592. https://doi.org/10.3923/jas.2008.3583.3592

Ali Belhocine, Mostefa bouchetara (2012). Thermal behavior of dry contacts in the brake discs. *International journal of automotive engineering*, Vol.3, PP 9-17. https://doi.org/10.20485/jsaeijae.3.1_9

Limpert Rudolf (1992). Brake Design and Safety. *Society of Automotive Engineers. Warrandale, Inc, Second Edition, USA*, PP 11-157.

Catalin Spulber, Stefan Voloaca (2012). Aspects regarding the disc brake's thermal stress simulation by using Infrared Thermography. *International Conference on Optimization of the Robots and Manipulators Romania, ISBN 978*, 26. https://doi.org/10.4028/www.scientific.net/amr.463-464.1197

Dr.Mushtaq Ismael Hasan (2011). Influence of Wall Axial Heat Conduction on The Forced Convection Heat Transfer In Rectangular Channels. *Basrah Journal for Engineering Science*, Vol.1, PP 31-43.

G. Babukanth, M.Vimla Teja (2012). Transient Analysis of Disk Brake by using ANSYS Software. *International Journal of Mechanical and Industrial Engineering*, Vol-2, PP 21-25. https://doi.org/10.47893/ijmie.2012.1082

Muhamad Ibrahim Mahmod, Kannan M. Munisamy (2011). Experimental analysis of ventilated brake disc with different blade configuration. *Department of Mechanical Engineering*, Vol. 1, PP 1-9.

Mr. Adarsh Bhat, Dr. Bhaskar Pal, Dr. Devendra Dandotiya (2021). Structural Analysis of a Two-Wheeler Disc Brake. *IOP Conference Series: Materials Science and Engineering*, Vol. 1. https://doi.org/10.1088/1757-899x/1013/1/012024

Cansu Ay (2021). *Disk Balata Çiftindeki Sıcaklık Dağılımının Frenleme Üzerine Etkisinin İncelenmesi*. [Yüksek lisans tezi, Marmara Üniversitesi]. YÖK Ulusal Tez Merkezi.

Yusuf Öncel (2020). *Fren Diskinin FEA(SEA) Analizi*. [Yüksek lisans tezi, İstanbul Gelişim Üniversitesi]. YÖK Ulusal Tez Merkezi.

Gökhan Keskin (2015). *Diskli Fren Sisteminde Disk Üzerindeki Sıcaklığın Analitik Olarak Hesaplanması*. [Yüksek lisans tezi, İstanbul Teknik Üniversitesi]. YÖK Ulusal Tez Merkezi.

Ahmet Mavi (2014). *Taşıt Frenlerinde Sıcaklık Etkisine Bağlı Olarak Fren Kuvveti Değişiminin Deneysel Olarak İncelenmesi*. [Yüksek lisans tezi, Afyon Kocatepe Üniversitesi]. YÖK Ulusal Tez Merkezi.

Yiğit Dalga (2018). *Taşıt Disk ve Fren Sıvı Sıcaklığının Tahmini İçin Bir Model Geliştirilmesi*. [Yüksek lisans tezi, İstanbul Teknik Üniversitesi]. YÖK Ulusal Tez Merkezi.

Öznur Çetin Giray (2020). *Otomotiv Fren Diski Tasarımı İçin Isı Transfer Karakteristiği İncelenmesi*. [Yüksek lisans, tezi, Yıldız Teknik Üniversitesi]. YÖK Ulusal Tez Merkezi.

Ezgi Ölgü (2020). *Taşıt Fren Sistemi Isıl Performansının Sayılsal İncelenmesi*. [Yüksek lisans tezi, Bursa Uludağ Üniversitesi]. YÖK Ulusal Tez Merkezi.

Yiğit Vatansever (2006). *Dört Akslı Bir Ağır Hizmet Aracına Ait Fren Sisteminin Bilgisayar Destekli Tasarımı ve Analizi*. [Yüksek lisans tezi, Dokuz Eylül Üniversitesi]. YÖK Ulusal Tez Merkezi.

Chetan Kumar Yadav, U.K.Joshi (2018). Structural and Thermal Analysis of Rotor Disc: A Review. *International Journal for Research Trends and Innovation*. https://doi.org/10.22214/ijraset.2018.6042

Ismail Bogrekci, Pinar Demircioglu, Emre Ceylan, Mehmet Kose, Mehmet Umut Kaya, (2024). Disc Brake Design and Analysis with Finite Element Methods. *The*

International Symposium for Production Research 2024 (ISPR2024). Springer Nature, Lecture Notes in Mechanical Engineering.

CURRICULUM VITAE

Surname, Name : CEYLAN Emre

Foreign Languages : English

E-mail :

Education

Degree	Institute	Graduation Date
MSc	Aydin Adnan Menderes University, Graduate School of Natural And Applied Sciences, Mechanical Engineering	Cont.
Bachelor	Karadeniz Teknik University, Engineering Faculty, Mechanical Engineering	2016

WORK EXPERIENCE

Year	Place/Institution	Title
2016-2021	Okt Trailer	R&D Engineer
2021-2024	EYS Endüstri Makina San. Ve Tic. A.Ş.	R&D Specialist
From 2024	Jantsa Jant San. ve Tic. A.ş.	R&D Specialist